



HAL
open science

Rab4b Deficiency in T Cells Promotes Adipose Treg/Th17 Imbalance, Adipose Tissue Dysfunction, and Insulin Resistance

Jérôme Gilleron, Gwennaëlle Bouget, Stoyan Ivanov, Cindy Meziat, Franck Ceppo, Bastien Vergoni, Mansour Djedaini, Antoine Soprani, Karine Dumas, Arnaud Jacquél, et al.

► **To cite this version:**

Jérôme Gilleron, Gwennaëlle Bouget, Stoyan Ivanov, Cindy Meziat, Franck Ceppo, et al.. Rab4b Deficiency in T Cells Promotes Adipose Treg/Th17 Imbalance, Adipose Tissue Dysfunction, and Insulin Resistance. *Cell Reports*, 2018, 25 (12), pp.3329-3341.e5. 10.1016/j.celrep.2018.11.083 . hal-01974357

HAL Id: hal-01974357

<https://hal.sorbonne-universite.fr/hal-01974357v1>

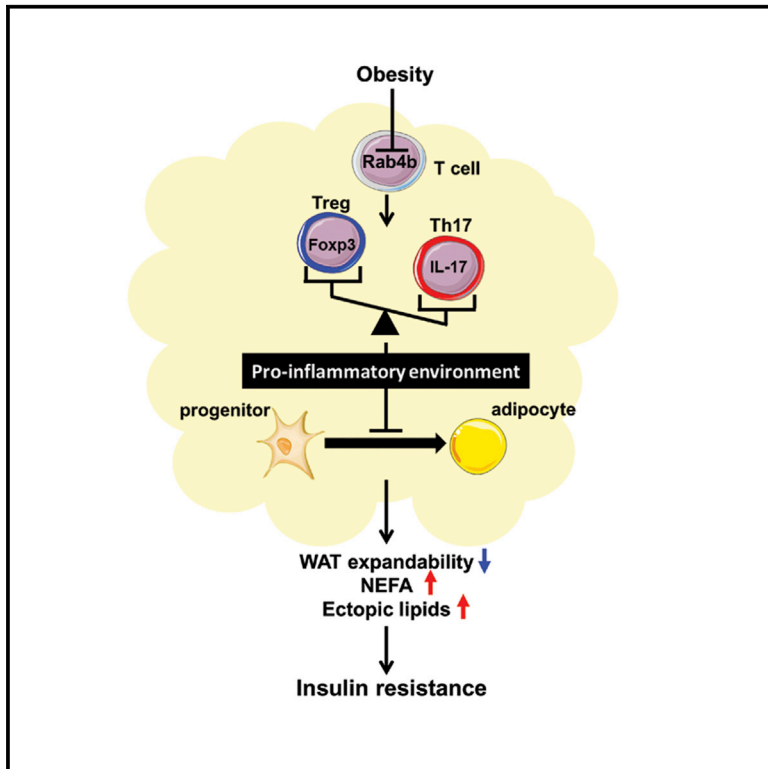
Submitted on 8 Jan 2019

HAL is a multi-disciplinary open access archive for the deposit and dissemination of scientific research documents, whether they are published or not. The documents may come from teaching and research institutions in France or abroad, or from public or private research centers.

L'archive ouverte pluridisciplinaire **HAL**, est destinée au dépôt et à la diffusion de documents scientifiques de niveau recherche, publiés ou non, émanant des établissements d'enseignement et de recherche français ou étrangers, des laboratoires publics ou privés.

Rab4b Deficiency in T Cells Promotes Adipose Treg/Th17 Imbalance, Adipose Tissue Dysfunction, and Insulin Resistance

Graphical Abstract



Authors

Jérôme Gilleron, Gwennaëlle Bouget, Stoyan Ivanov, ..., Nicolas Venteclef, Jean-François Tanti, Mireille Cormont

Correspondence

cormont@unice.fr

In Brief

Gilleron et al. show that Rab4b expression is decreased in adipose T cells during obesity in mice and humans. They reveal that Rab4b in T cells is critical for the control of adipose tissue remodeling and insulin sensitivity by regulating the adipose Th17/Treg balance.

Highlights

- Rab4b expression is decreased in adipose T cells of mice and patients with obesity
- Mice with a deficiency of Rab4b in T cells develop insulin resistance
- WAT expansion is impaired in mice with a deficiency of Rab4b in T cells
- Mice with a deficiency of Rab4b in T cells exhibit altered Th17/Treg balance



Rab4b Deficiency in T Cells Promotes Adipose Treg/Th17 Imbalance, Adipose Tissue Dysfunction, and Insulin Resistance

Jérôme Gilleron,^{1,2} Gwennaëlle Bouget,^{1,2} Stoyan Ivanov,^{2,3} Cindy Meziat,^{1,2} Franck Ceppo,^{1,2} Bastien Vergoni,^{1,2} Mansour Djedaini,^{1,2} Antoine Soprani,^{4,5} Karine Dumas,^{1,2} Arnaud Jacquel,^{2,6} Laurent Yvan-Charvet,^{2,3} Nicolas Venteclef,⁴ Jean-François Tanti,^{1,2} and Mireille Cormont^{1,2,7,*}

¹INSERM UMR1065, Mediterranean Center of Molecular Medicine C3M, Team “Cellular and Molecular Physiopathology of Obesity and Diabetes,” Nice, France

²Université Côte d’Azur, Nice, France

³INSERM U1065, Centre Méditerranéen de Médecine Moléculaire C3M, Team “Metabolism and Cancer,” Nice, France

⁴Sorbonne Université, Université Pierre et Marie Curie, INSERM, UMR S_1138 Cordeliers Research Center, Paris, France

⁵Clinique Geoffroy Saint-Hilaire, Ramsey Générale de Santé, Paris, France

⁶INSERM U1065, Centre Méditerranéen de Médecine Moléculaire C3M, Team “Cell Death, Differentiation, and Cancer,” Nice, France

⁷Lead Contact

*Correspondence: cormont@unice.fr

<https://doi.org/10.1016/j.celrep.2018.11.083>

SUMMARY

Obesity modifies T cell populations in adipose tissue, thereby contributing to adipose tissue inflammation and insulin resistance. Here, we show that Rab4b, a small GTPase governing endocytic trafficking, is pivotal in T cells for the development of these pathological events. Rab4b expression is decreased in adipose T cells from mice and patients with obesity. The specific depletion of Rab4b in T cells causes adipocyte hypertrophy and insulin resistance in chow-fed mice and worsens insulin resistance in obese mice. This phenotype is driven by an increase in adipose Th17 and a decrease in adipose Treg due to a cell-autonomous skew of differentiation toward Th17. The Th17/Treg imbalance initiates adipose tissue inflammation and reduces adipogenesis, leading to lipid deposition in liver and muscles. Therefore, we propose that the obesity-induced loss of Rab4b in adipose T cells may contribute to maladaptive white adipose tissue remodeling and insulin resistance by altering adipose T cell fate.

INTRODUCTION

White adipose tissue (WAT) plays an important role in regulating whole-body energy, glucose and lipid homeostasis, and insulin sensitivity through its metabolic and endocrine functions. The remodeling of WAT is a key homeostatic process that maintains the metabolic homeostasis in response to change in energy status (Pellegri-nelli et al., 2016; Rutkowski et al., 2015). Pathologic remodeling of WAT with alterations in its functions as in obesity is critically involved in the development of insulin resistance and obesity-related cardiometabolic disease. When WAT reaches its maximum capacity of expansion and becomes dysfunctional,

the ectopic accumulation of toxic lipids occurs in other metabolic organs as muscles and liver inhibiting insulin signaling and action (Hammarstedt et al., 2018).

The healthy and pathological expansion and function of WAT in response to metabolic cues depend on complex interplays between adipocytes and adipose stromal cells. Among these stromal cells, a delicate balance between pro- and anti-inflammatory immune cells, including macrophages and T cells, plays a key role in healthy WAT homeostasis through a fine-tuning of inflammatory signals (Boutens and Stienstra, 2016; Crewe et al., 2017; Fitzgibbons and Czech, 2016). Obesity alters both innate and adaptive immunity (Andersen et al., 2016). Obesity shifts adipose innate immune cells toward a pro-inflammatory state with an increase in metabolically and/or classically activated macrophages (Boutens and Stienstra, 2016). This is accompanied by the production of pro-inflammatory mediators that impair insulin signaling and the functions of insulin-sensitive tissues, but also affect WAT expansion and adipocyte differentiation (Hammarstedt et al., 2018; Tanti et al., 2013). Different lymphocyte subsets are also modified in WAT from subjects with obesity. Among them, regulatory T cells (Tregs) are decreased, whereas effector T cells increased, and this imbalance participates in WAT inflammation and dysfunction (Feuerer et al., 2009; Priceman et al., 2013; Winer et al., 2009). It is therefore clear that cross-talk between immune cells and adipocytes is crucial for WAT homeostasis and that a deregulation of this cross-talk contributes to the pathological remodeling of WAT, but the underlying cellular and molecular mechanisms remain incompletely understood.

Endocytosis is critically involved in cell adaptation to external cues, including metabolic ones, and in the cross-talk between different cell types within tissues by controlling the subcellular localization of protein complexes in a microenvironment-dependent manner (Di Fiore and von Zastrow, 2014). The family of Rab guanosine triphosphatases (GTPases) is a central hub governing intracellular trafficking through membrane tethering, fusion, and motility (Galvez et al., 2012). We and others have shown that



Rabs, including the Rab4 family, control the insulin-induced glucose transporter Glut4 translocation to the plasma membrane in adipocytes (Cormont et al., 1996; Mari et al., 2006). In particular, we identified Rab4b, an endosomal Rab, as a key player in Glut4 translocation in adipocytes, and more important, the expression of Rab4b was decreased in the WAT of obese and insulin-resistant mice and in patients affected by obesity (Kaddai et al., 2009). In addition to being expressed in adipocytes, Rab4b is strongly expressed in immune cells (Gurkan et al., 2005), and a fine-tuned intracellular trafficking controls the function and fate of the immune cells (Pei et al., 2012). Therefore, it was plausible that a deregulation of Rab4b expression in adipose immune cells participates in the alteration of WAT remodeling and functions.

We show here that Rab4b expression was reduced in the adipose T cells of obese mice and patients with obesity, but not in adipocytes. To address the pathophysiological importance of this decrease, we generated mice with a specific invalidation of Rab4b in T cells. We demonstrate that Rab4b invalidation in T cells worsened the insulin resistance of diet-induced obese mice and was enough to promote the glucose intolerance and insulin resistance of mice fed a normal chow diet (NCD). This was due to unhealthy WAT expansion and inflammation, leading to ectopic lipid deposits in liver and muscles. WAT inflammation started early, with a decrease in Treg cells and an increase in T helper cell 17 (Th17) in adipose tissue. We also show that the loss of Rab4b in T cells skewed Th0 differentiation toward Th17 at the expense of Treg. Thus, we identify Rab4b in T cells as a critical factor in the control of WAT remodeling and insulin sensitivity by regulating T cell function and fate.

RESULTS

Rab4b mRNA Levels Are Reduced in CD3⁺ T Lymphocytes from the Adipose Tissue of Subjects with Obesity

We previously reported that the level of *Rab4b* mRNA was reduced in WAT from patients with obesity and type 2 diabetes and in epididymal WAT (epiWAT) from *db/db* mice (Kaddai et al., 2009). Here, we found a progressive decrease in *Rab4b* mRNA expression in epiWAT when the percentage of calories from lipids in the diet increased from 8.4% (NCD) to 45% and 60% (high-fat diet [HFD]) after 16 weeks (Figure 1A). The *Rab4b* mRNA expression in epiWAT was inversely correlated to fasting glucose, fat pad weight, and the glucose tolerance index (Figure 1B). The decrease in Rab4b expression was detected after 4 weeks of 60% HFD (Figure 1C), and an inverse correlation with fasting glucose, adipocyte size, and the glucose tolerance index was already present (Figure 1D). These results suggest a link between the low levels of Rab4b in epiWAT and alterations in glucose homeostasis in obesity. The *Rab4b* mRNA level was unchanged in adipocytes between lean and obese mice (Figure 1E), whereas it was decreased by 30% in epiWAT CD3⁺ T lymphocytes from obese mice compared to lean mice (Figure 1F). More important, *Rab4b* mRNA expression was also decreased in human CD3⁺ T lymphocytes isolated from visceral WAT of non-diabetic patients with obesity compared to individuals without obesity (BMI <30), and this

reduction was even stronger when the patients with obesity were also diabetic, reaching a 2-fold decrease compared to non-obese individuals (Figure 1G; Table S1). The level of Rab4b expression was inversely correlated to BMI, fasting glucose, and hemoglobin A1c (HbA1c) and positively correlated to high-density lipoprotein (HDL) cholesterol (Table S2). These results demonstrate that the level of *Rab4b* mRNA decreases in the T lymphocytes of WAT in mice and patients affected by obesity.

Generation of Mice with a Specific Invalidation of Rab4b in T Cells

To investigate the results of the reduced Rab4b expression in T cells on glucose and lipid homeostasis and insulin resistance, we generated mice in which the *Rab4b* gene was disrupted by homologous recombination specifically in T cells (Rab4b^{Tcell KO} mice) by crossing mice with *Rab4b* floxed alleles (Rab4b^{flox/flox} mice), with mice expressing the Cre recombinase under the control of the promoter of the T lymphocyte-specific protein tyrosine kinase Lck (Lck-Cre mice) (Figures 2A, S1A, and S1B). As anticipated, *Rab4b* mRNA expression was markedly reduced in T lymphocytes and in natural killer (NK)/NKT cells isolated from the spleen of Rab4b^{Tcell KO} mice, but not in monocytes and B lymphocytes (Figure 2B). Reduced mRNA expression of *Rab4b* was consistently observed in the spleen of Rab4b^{Tcell KO} mice, which is enriched in T lymphocytes, but not in other organs such as the brain, muscle, or liver (Figure S1C). The knockdown efficiency was also validated by western blot (Figure 2C). The expression of other endocytic Rabs, including the Rab4b homologous Rab4a and Rab5a, Rab11a, and Rab14, were unchanged (Figure S1D). Since lymphocytes are present in WAT, we reasoned that the expression of Rab4b should be decreased in the stroma vascular fraction (S_F). Accordingly, the *Rab4b* mRNA expression was decreased by ~50% in the S_F of epiWAT, and no change was found in adipocytes (Figure 2B). These findings indicate that the mice with the Rab4b deletion in lymphocytes are suitable for studying the consequences of a decreased expression of Rab4b in adipose T cells on metabolic disorders associated with obesity.

Loss of Rab4b in T Cells Causes Glucose Intolerance and Insulin Resistance with Aging in Chow-Fed Mice and Worsens Insulin Resistance in Obesity

To determine whether the reduced expression of *Rab4b* mRNA in adipose tissue lymphocytes during obesity is linked to metabolic complications, Rab4b^{Tcell KO} mice were studied under an NCD for 35 weeks or challenged with an HFD (60% energy from fat) from the age of 7 weeks for 18 weeks. Rab4b^{Tcell KO} mice gained similar weight and fat mass as their littermate controls both on NCD (Figures 3A and 3B) and after HFD (Figures 3C and 3D). At 10 weeks of age, random-fed glucose and insulin levels were not different in chow-fed animals (Figures 3E and 3F). However, at 25 and 35 weeks of age, chow-fed Rab4b^{Tcell KO} had a 2- to 3-fold increase in random-fed serum insulin levels (Figure 3F) and abnormal plasma glucose levels in the fasting state (Rab4b^{flox/flox} versus Rab4b^{Tcell KO}: 179.0 ± 10.9 and 214.2 ± 9.3; p < 0.05 in 25-week-old mice; 179.5 ± 7.4 and 203.1 ± 4.3; p < 0.05 in 35-week-old mice). These findings

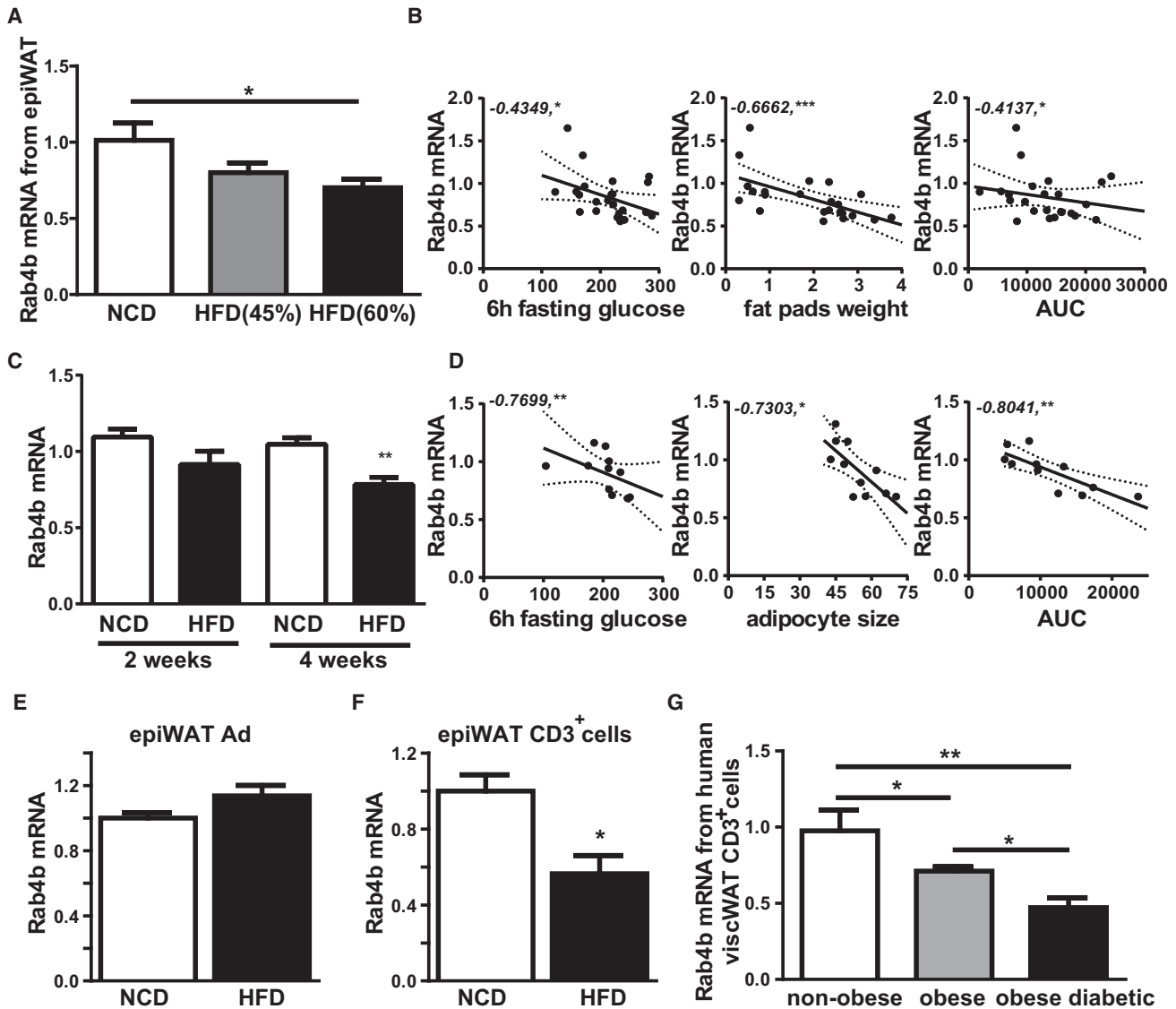


Figure 1. Rab4b Expression Is Reduced in CD3⁺ Lymphocytes from Mice and Human Adipose Tissue in Obesity

(A) Rab4b mRNA level in epiWAT of mice (n = 8/group) fed NCD or HFD (45% or 60%) for 16 weeks.

(B) The linear regression best fits with 95% confidence are shown.

(C) Rab4b mRNA level in epiWAT of mice fed NCD or 60% HFD for 2 or 4 weeks (Vergoni et al., 2016).

(D) The linear regression best fits with 95% confidence are shown.

(E) Rab4b mRNA in adipocytes isolated from epiWAT of mice (n = 8) fed NCD or 60% HFD.

(F) Rab4b mRNA in CD3⁺ cells of epiWAT S_F of mice fed NCD or HFD (n = 4/group). The S_F from two mice were pooled for CD3⁺ cell isolation.

(G) Rab4b mRNA in CD3⁺ cells from visceral adipose tissue (VAT) of patients without obesity (n = 4), patients with obesity (n = 10), and patients with obesity and type 2 diabetes (n = 10).

Graphs show means ± SEMs. Statistical significance is shown as *p < 0.05, **p < 0.01, and ***p < 0.001.

revealed the first signs of metabolic complications. Although chow-fed Rab4b^{Tcell KO} mice did not reveal differences on glucose tolerance compared to controls at 25 weeks of age on an intraperitoneal glucose tolerance test (ipGTT) (Figures 3G and S2A), 35-week-old Rab4b^{Tcell KO} mice remarkably developed glucose intolerance (Figures 3H and S2A). Compared to chow-fed Rab4b^{flx/flx} littermates, Rab4b^{Tcell KO} mice also exhibited higher plasma insulin concentrations at the 20-min time

point after glucose challenge (Figure 3I) and a 2-fold increase in the homeostasis model assessment of insulin resistance ([HOMA-IR] 2.9 ± 0.4 for Rab4b^{flx/flx} mice versus 6.1 ± 0.9 for Rab4b^{Tcell KO} mice; p = 0.03). Accordingly, Akt phosphorylation on Thr308 and Ser473 was decreased in the muscle of 35-week-old Rab4b^{Tcell KO} mice (Figure 3J; phosphorylated AKT-308 [pAKT-308]: 0.95 ± 0.05 for Rab4b^{flx/flx} mice versus 0.75 ± 0.05; p = 0.052, and pAKT-473: 1.02 ± 0.07 for

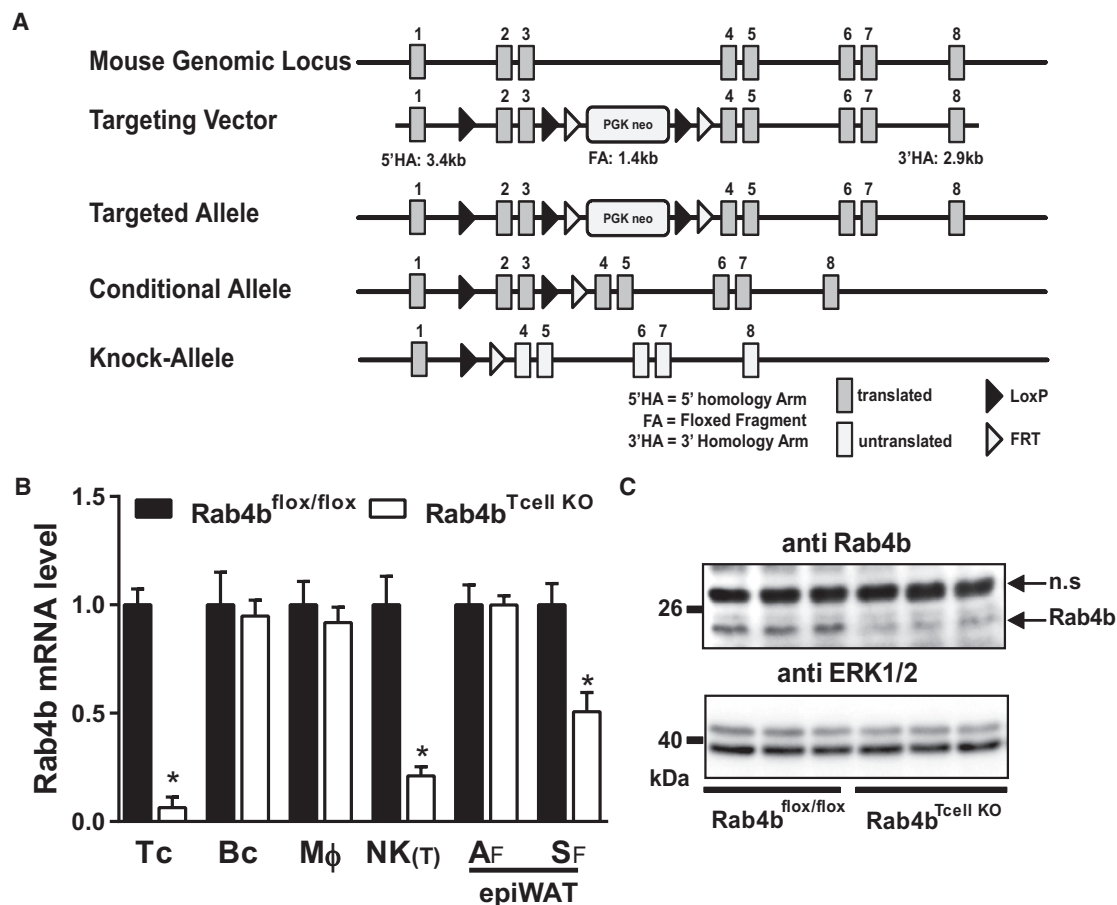


Figure 2. T Cell-Specific Invalidation of the *Rab4b* Gene in Mice

(A) Schematic representation of the strategy.

(B) *Rab4b* mRNA expression in Tc: CD3⁺ T cell, Bc: B220⁺ B cell, Mφ: CD11b⁺ monocyte, NK(T): NK1.1⁺ cell, Af: adipocyte fraction, Sf: stromal vascular fraction of epiWAT (n = 6/genotype). mRNA levels are relative to mouse *RPLP0*.

(C) Immunoblot of Rab4b in thymus lysate of Rab4b^{flox/flox} and Rab4b^{Tcell KO} mice with extracellular signal-regulated kinase (ERK)1/2 as control.

Rab4b^{flox/flox} mice versus 0.70 ± 0.07 ; $p < 0.05$). To verify that this change in glucose homeostasis was not due to the Lck-Cre transgene, we compared Lck-Cre mice with Rab4b^{flox/flox} and wild-type (WT) mice at 35 weeks of age. We did not observe differences in glucose tolerance, fed and fasted blood glucose, fed blood insulin, and fat mass in those mice (Figures S2C–S2H). We then investigated the metabolic phenotype of the Rab4b^{Tcell KO} mice fed an HFD. After 15 weeks of HFD feeding, Rab4b^{Tcell KO} mice showed not only a 2.5-fold increase in random-fed serum insulin level with similar random-fed glucose compared to Rab4b^{flox/flox} littermates (Figures 3K and 3L) but also an increase in fasting blood glucose (213.5 ± 29.6 for Rab4b^{flox/flox} mice versus 279.5 ± 10.2 for Rab4b^{Tcell KO} mice; $p < 0.05$). These were associated with the development of a more severe glucose intolerance, with a 2-fold increase in the area under the curve on ipGTT (Figures 3M and S2B) and a worse insulin resistance by insulin tolerance test (Figure 3N). These findings show that Rab4b deficiency in T cells drives, without altering body weight and adipose mass, a progressive alteration in glucose tolerance

and insulin response with age in mice fed an NCD and worsens glucose intolerance and insulin resistance upon HFD.

Rab4b^{Tcell KO} Mice Display Ectopic Lipid Accumulation and an Increase in Circulating Level of Non-esterified Fatty Acids

The NCD-fed Rab4b^{Tcell KO} mice at 35 weeks of age developed dyslipidemia with a significant increase in blood levels of non-esterified fatty acids (NEFAs) in the fasting state (Figure 4A) and 5.6- and 3.5-fold increases in muscle and liver triglycerides (TGs) content, respectively (Figures 4B and 4C). These findings clearly correlated with the glucose intolerance these mice developed. An increase in circulating NEFAs was also observed at 25 weeks of age, when features of metabolic complications start to occur, but without signs of ectopic lipid deposits in muscle and liver (Figures 4B and 4C). At this age, Rab4b^{Tcell KO} mice exhibited a lower respiratory quotient (RQ) compared to Rab4b^{flox/flox} mice, mainly in the light phase (Figures 4D and 4E), as compared to control mice without

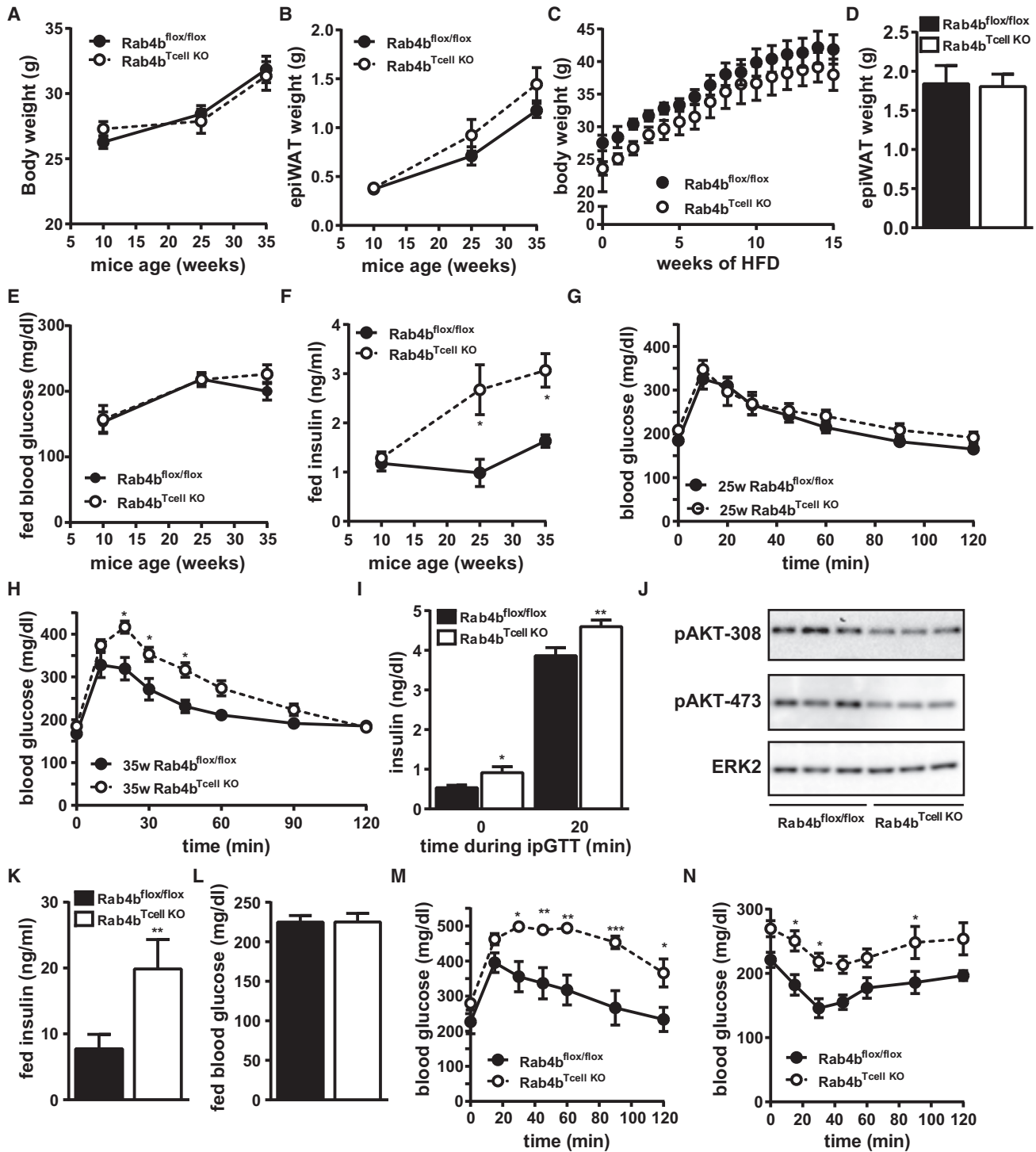


Figure 3. T Cell-Specific Invalidation of Rab4b Causes Glucose Intolerance and Insulin Resistance with Aging in Chow-Fed Mice and Worsens Insulin Resistance in the Obese State

Rab4b^{flox/flox} and Rab4b^{Tcell KO} mice were fed an NCD and studied at 10 weeks (n = 6/genotype), 25 weeks (n = 8/genotype), and 35 weeks (n = 8/genotype) of age (A, B, and E–J) or a 60% HFD for 18 weeks from the age of 7 weeks (n = 6/genotype) (C, D, and K–M).

(A and C) Body weight curve of mice under NCD (A) and HFD (C).

(B and D) EpiWAT weight of mice under NCD (B) and HFD (D).

(E and L) Random-fed blood glucose of mice under NCD (E) and HFD (L).

(F and K) Random-fed serum insulin of mice under NCD (F) and HFD (K).

(legend continued on next page)

modifications in energy expenditure, activity, and rearing (Figures S3A–S3F). This is indicative of higher lipid utilization and can explain the lack of ectopic lipid accumulation, despite the increase in circulating NEFAs in 25-week-old Rab4b^{Tcell KO} mice. Upon HFD, Rab4b^{Tcell KO} mice experienced a worsening of liver steatosis, with an increase in both lipid droplet number and size (Figures 4F and 4G). These results indicate that Rab4b deficiency in T cells induced ectopic lipid accumulation with age in mice fed an NCD and worsens liver steatosis upon HFD challenge.

Loss of Rab4b in T Lymphocytes Drives Pathological Adipose Tissue Expansion with Enlarged Adipocytes

The increase in fasting blood NEFAs followed by the ectopic lipid deposits in chow-fed Rab4b^{Tcell KO} mice suggests that the glucose intolerance and metabolic abnormalities may originate from alterations in WAT functions. To determine whether loss of Rab4b in T cell drives WAT alterations, we analyzed adipose tissue cellularity and adipocyte size. Despite no change in epiWAT mass between the two genotypes (Figure 3B), there was a 30% increase in the mean diameter of adipocytes from chow-fed Rab4b^{Tcell KO} mice compared to Rab4b^{flox/flox} littermates as early as 25 weeks of age, when features of metabolic complications started to occur (Figures 5A and 5B). By contrast, adipocyte size was unaltered in 10-week-old Rab4b^{Tcell KO} mice that did not exhibit metabolic alterations (Figures 5A, 5B, and S4A). Accordingly, the expression of leptin mRNA that is tightly correlated with adipocyte size (Guo et al., 2004) was increased in the epiWAT of 35-week-old Rab4b^{Tcell KO} mice, but not in the epiWAT and isolated adipocytes of 10-week-old Rab4b^{Tcell KO} mice (Figures 5C and S4B). Adipocytes from 10-week-old Rab4b^{flox/flox} and Rab4b^{Tcell KO} mice also expressed similar levels of glucose transporter type 4 (GLUT4) and uncoupling protein 1 (UCP1) in epiWAT and subcutaneous white adipose tissue (scWAT) (Figure S4B). Because of the increase in fasting blood NEFAs in Rab4b^{Tcell KO} mice, we looked at the expression of genes controlling adipocyte lipolysis in epiWAT. We found decreased perilipin (*PLIN1*) mRNA in epiWAT from chow-fed Rab4b^{Tcell KO} mice (Figure 5C). By contrast, the mRNA expression of the lipases adipose triglyceride lipase (ATGL), hormone-sensitive lipase (HSL), and monoacylglycerol lipase (MGL) was unaltered (Figure 5C). However, the phosphorylation of the activating protein kinase A (PKA)-dependent phosphorylation site S563 on HSL was increased by 1.8-fold (Figure 5D). A decrease in *PLIN1* and an increase in S563-HSL support an increase in epiWAT lipolytic activity, which could explain the increase in plasma NEFAs in Rab4b^{Tcell KO} mice. Our findings illustrate that the loss of Rab4b in T cells promotes the development of hypertrophic and dysfunctional adipocytes in the epiWAT of Rab4b^{Tcell KO} mice, a feature of unhealthy WAT that is associated with insulin resistance and metabolic complications (Crewe et al., 2017; Hammarstedt et al., 2018).

Loss of Rab4b in T Cells Promotes Early Impairment in Adipogenesis Affecting the Dynamic of Adipose Tissue Expansion

The unaltered epiWAT mass observed in Rab4b^{Tcell KO} mice, together with the increase in adipocyte size, suggested fewer adipocytes. Consistent with this hypothesis, the calculated number of adipocytes, although similar between the two genotypes until 10 weeks of age, plateaued earlier in Rab4b^{Tcell KO} mice than in their control littermates. Consequently, the number of mature adipocytes was halved in 25- or 35-week-old Rab4b^{Tcell KO} mice compared with Rab4b^{flox/flox} mice (Figure 5E). The number of adipocytes in scWAT was also decreased in 35-week-old Rab4b^{Tcell KO} mice, although the adipocyte size remained unchanged in accordance with the trend in the decreased scWAT weight.

Because pathological fat mass expansion can result from limited recruitment and differentiation of adipocytes from progenitor cells (Hammarstedt et al., 2018), we determined whether the alteration in the dynamic of epiWAT expansion in Rab4b^{Tcell KO} mice resulted from a reduction in adipocyte differentiation from their progenitors. First, we tried to determine whether Rab4b deficiency in T lymphocytes affected the number of mesenchymal stem cells (MSCs) within the epiWAT, because adipose MSCs are committed into preadipocytes before being differentiated into mature adipocytes. We studied the epiWAT from 10-week-old mice to detect early defects. The S_F of the epiWAT from 10-week-old Rab4b^{flox/flox} and Rab4b^{Tcell KO} mice was cultured under conditions favoring only the growth of the MSCs, and the number of MSC colony-forming units (CFUs) was quantified (Figure 5F). The CFU number was increased by almost 2-fold in the Rab4b^{Tcell KO} mice, suggesting an early defect in preadipocyte commitment. The capacity of the epiWAT MSCs (Figure S4C) and preadipocytes (Figure S4D) from 10-week-old Rab4b^{Tcell KO} mice to differentiate into adipocytes *ex vivo* was unaltered, suggesting that factors secreted in the adipose tissue microenvironment of the Rab4b^{Tcell KO} mice altered MSC-derived preadipocyte commitment and differentiation. To address this possibility, 3T3-L1 preadipocytes were induced to differentiate into adipocytes in the presence of the epiWAT explants from 10-week-old Rab4b^{Tcell KO} or Rab4b^{flox/flox} mice. EpiWAT explants from Rab4b^{Tcell KO} mice reduced by 60% 3T3-L1 differentiation in adipocyte compared to explants from Rab4b^{flox/flox} mice, as shown by reduced TG accumulation visualized by oil red O staining and by the reduced expression of adipocyte-specific genes (Figure 5G). These data demonstrate that the hypertrophic phenotype of adipocytes is associated with an early impairment in adipogenesis and suggest that the loss of Rab4b in T cell promotes, as early as 10 weeks of age, an epiWAT microenvironment that restricts adipocyte differentiation. This alteration in the dynamic of WAT expansion occurs before the development of the metabolic complications of the Rab4b^{Tcell KO} mice.

(G, H, and M) Intraperitoneal glucose tolerance test of 25-week-old mice under NCD (G), 35-week-old mice under NCD (H), and 25-week-old mice under HFD (M).
(I) Serum insulin during the ipGTT in 35-week-old mice.

(J) Representative western blot of muscle AKT phosphorylation in 35-week-old mice under NCD with ERK2 used as control.

(N) Insulin tolerance test in mice fed HFD.

Values are means ± SEMs. Statistical significance is shown as *p < 0.05, **p < 0.01, and ***p < 0.001.

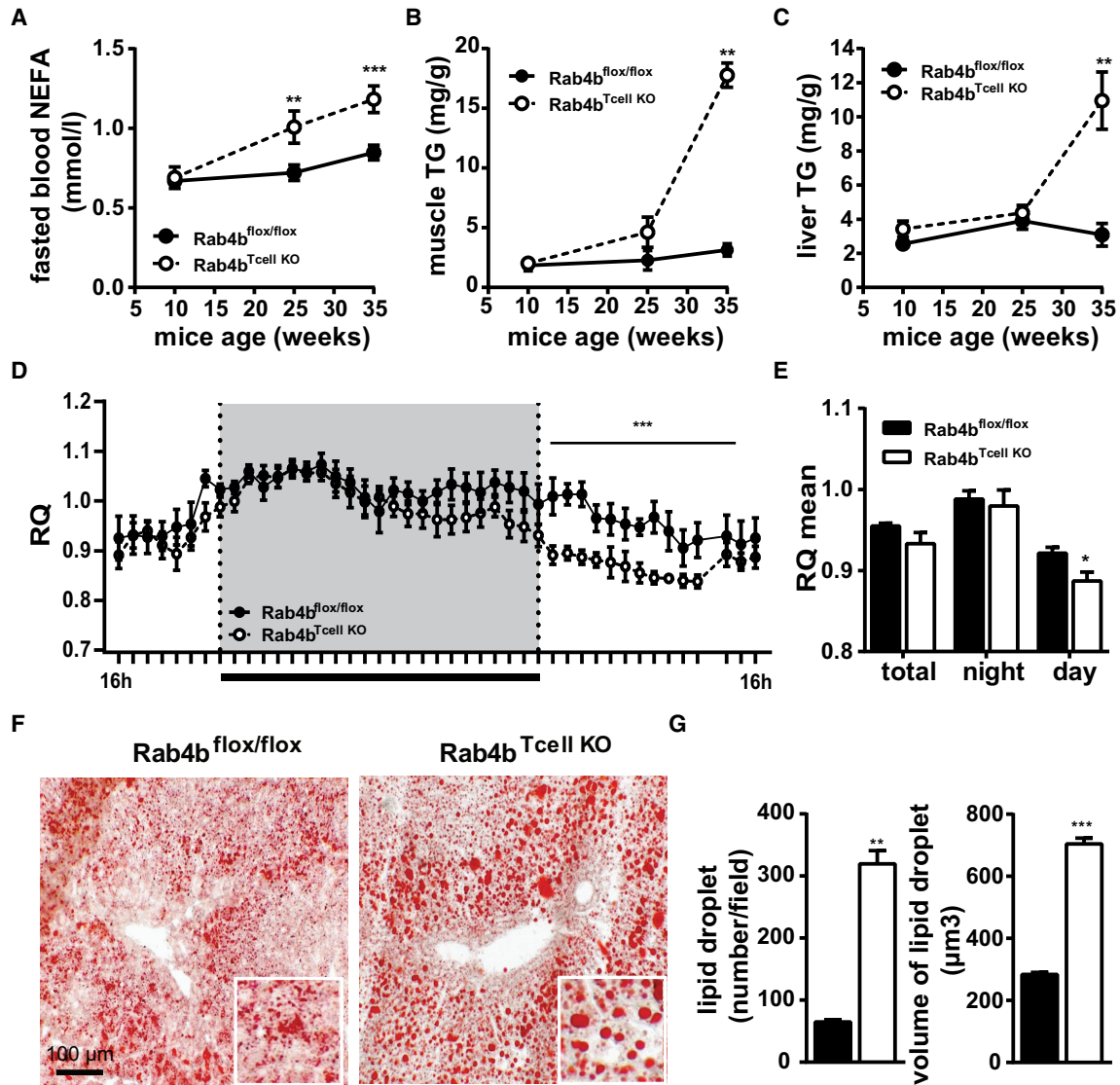


Figure 4. T Cell-Specific Invalidation of Rab4b Induced Ectopic Lipid Accumulation and an Increase in the Circulating Level of Non-esterified Fatty Acids

Rab4b^{flx/flx} and Rab4b^{Tcell KO} mice were fed an NCD and studied at 10 weeks (n = 6/genotype), 25 weeks (n = 8/genotype) and 35 weeks (n = 8/genotype) of age (A–E) or fed a 60% HFD for 18 weeks from the age of 7 weeks (n = 6/genotype) (F and G).

(A) Circulating NEFA after 6 hr of fasting.

(B and C) TG content in muscles (B) and liver (C) of random-fed mice.

(D) Respiratory quotients (RQs) in 25-week-old Rab4b^{flx/flx} and Rab4b^{Tcell KO} mice randomly fed with NCD.

(E) Mean RQ in night and day periods.

(F) Oil red O staining of liver section.

(G) Quantification of liver lipid droplets.

Values are means ± SEMs. Statistical significance is shown as *p < 0.05, **p < 0.01, and ***p < 0.001.

Loss of Rab4b in T Cells Promotes WAT Inflammation in Chow-Fed Mice

Adipocyte function and differentiation are controlled by the inflammatory environment (Hammarstedt et al., 2018). Thus, to determine whether the loss of Rab4b in T cells impaired adipogenesis through an alteration of the epiWAT cytokine secretion profile, we screened for cytokines and/or chemokines that are

differentially secreted by the explants of 10-week-old Rab4b^{Tcell KO} and Rab4b^{flx/flx} mice. Cytokine and/or chemokine array analysis revealed that explants from 10-week-old Rab4b^{Tcell KO} mice secreted higher amounts of cytokines such as interleukin-17A (IL-17A), IL-6, and IL-1 α or chemokines such as C-X-C motif chemokine ligand 5 (CXCL5) and CXCL12 and lower amounts of C-C motif chemokine ligand 5 (CCL5)

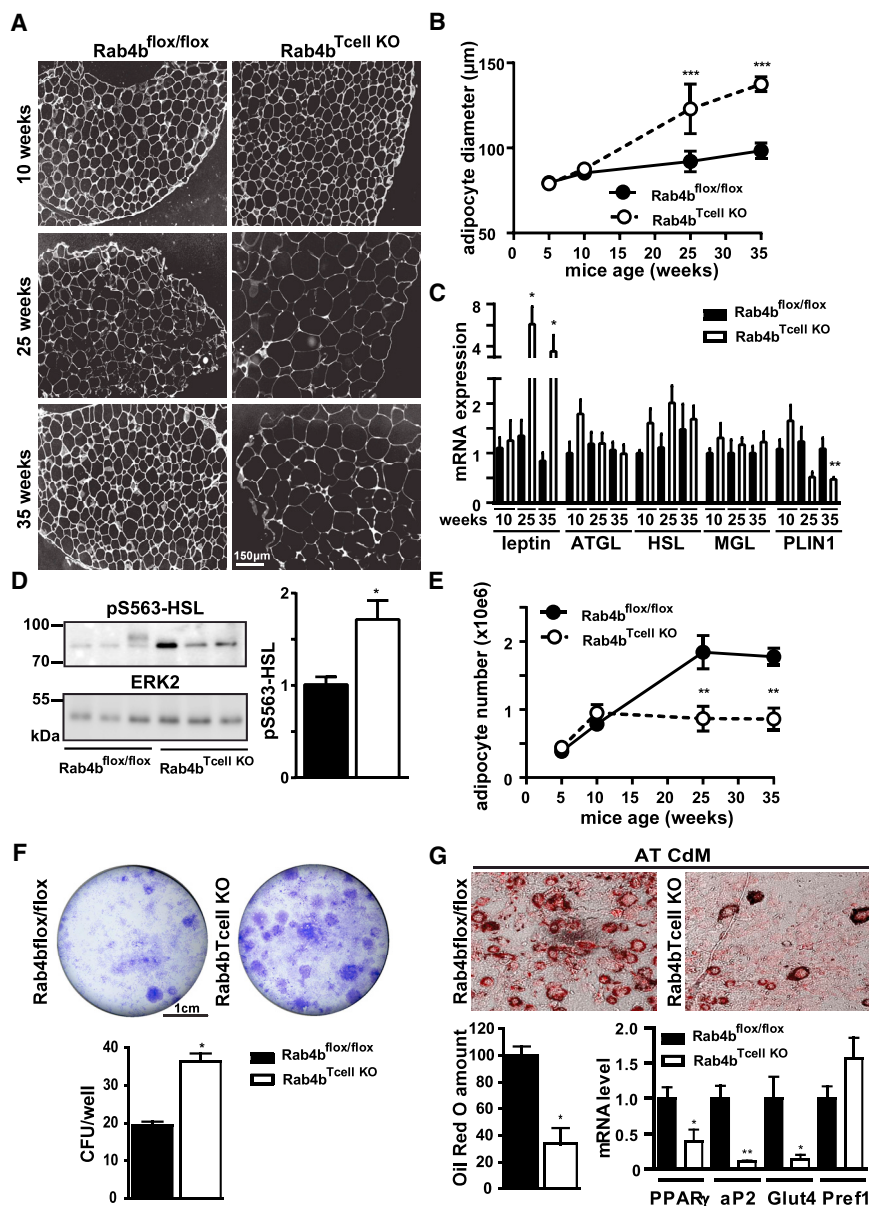


Figure 5. T Cell-Specific Invalidation of Rab4b Affects Adipose Tissue Homeostasis and Promotes an Early Impairment in Adipogenesis

Rab4b^{flox/flox} and Rab4b^{Tcell KO} mice were fed an NCD and studied at 10 weeks (n = 6/genotype), 25 weeks (n = 8/genotype), and 35 weeks (n = 8/genotype) of age.

(A and B) Representative images (A) and quantification (B) of adipocyte diameters in epiWAT.

(C) Expression levels of mRNA in epiWAT from random-fed mice (n = 6/genotype) at 10 and 35 weeks of age. The level of mRNAs is relative to *RPLP0* and is expressed relative to Rab4b^{flox/flox} mice at each age.

(D) Representative western blot and quantification (n = 6/genotype) of HSL phosphorylation on Ser563 in the epiWAT of 35-week-old mice under an NCD with ERK2 as control.

(E) Mathematical estimation of the adipocyte number in epiWAT.

(F) Representative image and quantification of MSC colony-forming units (CFUs) in the S_F of 10-week-old Rab4b^{flox/flox} and Rab4b^{Tcell KO} mice (n = 12 preparations of S_F).

(G) Representative image and lipid quantification by oil red O staining in 3T3-L1 adipocytes differentiated in the presence of explants of epiWAT of 10-week-old Rab4b^{flox/flox} and Rab4b^{Tcell KO} mice (n = 6 explants). Values are means ± SEMs. Statistical significance is shown as *p < 0.05, **p < 0.01, and ***p < 0.001.

(Figures 6A and 6B). IL-17A, IL-6, and IL-1 α are cytokines that are known to inhibit adipocyte differentiation (He et al., 2006; Rotter et al., 2003; Shin et al., 2009; Zúñiga et al., 2010). The mRNA expression of IL-17A, IL-6, CXCL5, and CXCL12 was also consistently increased in the epiWAT of 10-week-old Rab4b^{Tcell KO} mice, while that of CCL5 was decreased and that of IL-2 and IL-10 was unchanged (Figure 6C). This inflammatory signature in Rab4b^{Tcell KO} mice suggested an early imbalance in adipose tissue T cell homeostasis that can be at the origin of the alteration in epiWAT expandability.

Rab4b Deficiency in T Cells Induces an Early Increase in Adipose Th17 and a Decrease in Adipose Treg

To determine whether the observed changes in cytokine secretion could be due to changes in the populations of adipose

immune cells because of the loss of Rab4b in T cells, we characterized adipose immune cells in the epiWAT of 10- and 35-week-old Rab4b^{flox/flox} and Rab4b^{Tcell KO} mice by flow cytometry by using the gating strategies described in Figure S5. The proportion of CD4⁺ and CD8⁺ T lymphocytes as well as adipose NKT cells relative to conventional T cells in epiWAT cells was similar in the two genotypes whatever the age of the mice (Figures 7A and S6A). The number

of $\gamma\delta$ T, NK, and B cells did not differ in epiWAT between the two genotypes at 10 and 35 weeks of age (Figures S6A and S6B). The invalidation of Rab4b in T cells did not affect adipose memory T cells in the epiWAT (Figure S7), which could have disturbed adipose tissue metabolic functions, as described by Han et al. (2017). Thus, because we observed an increase in IL-17A production by the epiWAT from Rab4b^{Tcell KO} mice, we assessed whether the number of IL-17A-producing cells was changed. The number and proportion of IL-17A⁺ T cell receptor β positive (TCR β ⁺) was increased by ~2.5-fold in the epiWAT of 10- and 35-week-old Rab4b^{Tcell KO} mice compared to age-matched Rab4b^{flox/flox} mice (Figure 7B). A similar increase occurred in the scWAT of 10-week-old Rab4b^{Tcell KO} mice (Figure S8A). The number of IL-17A-producing $\gamma\delta$ T or NK cells was not different between the two genotypes whatever the age of

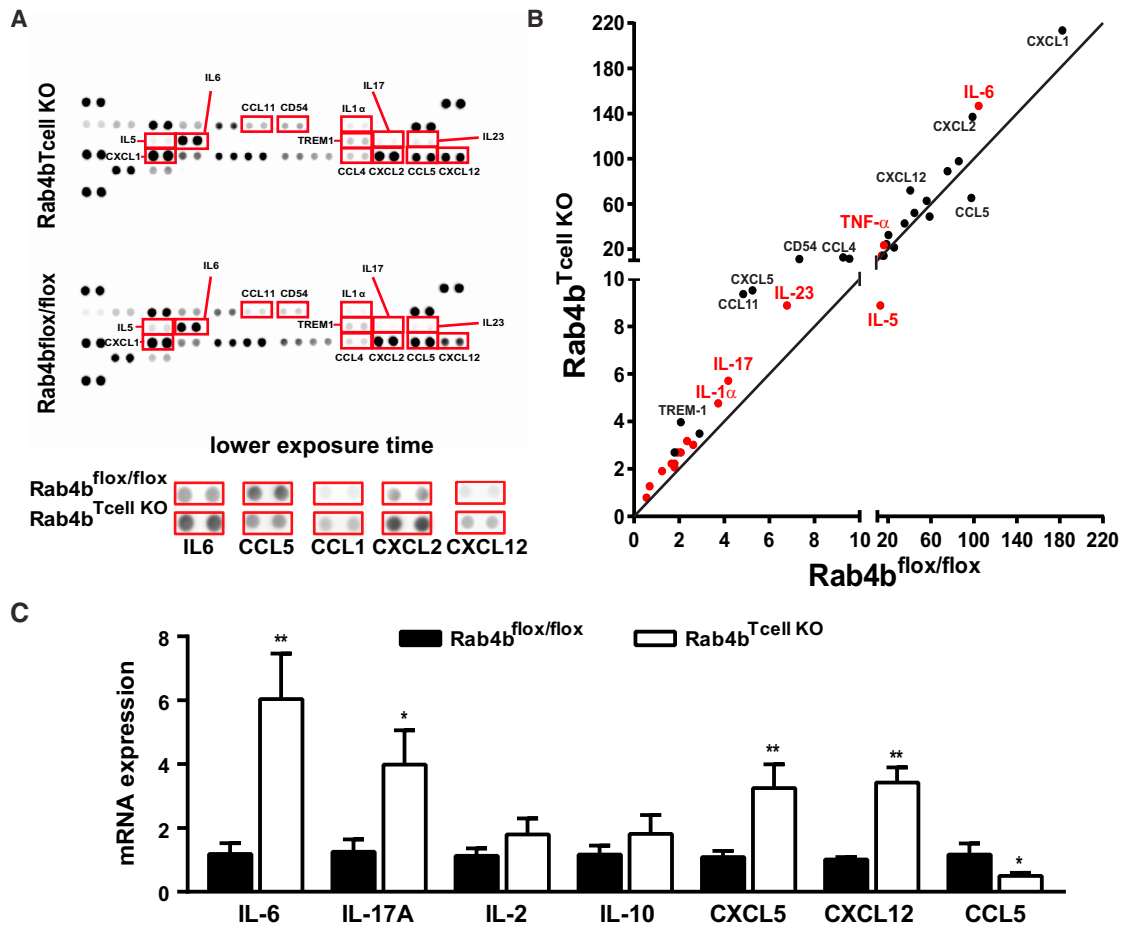


Figure 6. T Cell-Specific Invalidation of Rab4b in T Cells Promotes WAT Inflammation in Chow-Fed Mice

(A and B) Secretion of epiWAT explants from 10-week-old Rab4b^{flox/flox} and Rab4b^{Tcell KO} mice analyzed using a cytokine and/or chemokine array (A) and quantified (B). Black dots, chemokines; red dots, cytokines.

(C) Expression levels of cytokine and/or chemokine mRNA in the epiWAT of 10-week-old Rab4b^{flox/flox} and Rab4b^{Tcell KO} mice (n = 6/genotype). The level of mRNAs is relative to *RPLP0*.

Values are means ± SEMs. Statistical significance is shown as *p < 0.05 and **p < 0.01.

the mice (Figure S6C). The expression of IL-17A in Th17, $\gamma\delta$ T, or NK cells was the same between 10- or 35-week-old Rab4b^{flox/flox} and Rab4b^{Tcell KO} mice (Figure S6D). Conventional T cells (TCR $\alpha\beta$) were the major subtypes of IL-17A-expressing immune cells (Figure S8B), and most of them were CD4⁺ T cells (Figure S8C). The increase in Th17 in the epiWAT of Rab4b^{Tcell KO} mice was associated with a decrease in the proportion and number of Foxp3-expressing Treg cells (Figure 7C), suggesting that Rab4b deficiency in T cells induced an early alteration in the Th17/Treg balance within the epiWAT, which can progressively lead to a more profound alteration in adipose tissue inflammation with age. Accordingly, compared to Rab4b^{flox/flox} mice at 35 weeks of age, age-matched Rab4b^{Tcell KO} mice displayed a 1.5-fold increase in F4/80⁺ macrophages and a higher mRNA expression of F4/80 in epiWAT (Figures S6E and S6F), with an ~1.4-fold increase in pro-inflammatory F4/80^{high}CD11c^{high} macrophages but no differences in the number of F4/80^{low}CD11c^{high} cells (Figure S6E). This increase in macrophage infiltration was

associated with an increase in the mRNA expression of CCL2 and tumor necrosis factor α (TNF- α) (Figure S6F).

Rab4b Deficiency Induces a Cell-Autonomous Defect in T Cell Polarization

To determine whether the alteration in the Th17/Treg balance in Rab4b^{Tcell KO} mice was cell autonomous, naive splenic CD4⁺CD62L^{high}CD44^{low} T cells (Th0 cells) from Rab4b^{flox/flox} and Rab4b^{Tcell KO} mice were differentiated *in vitro* either in Treg or in Th17. Of note, Rab4b expression was not affected during Treg/Th17 differentiation and appeared similar whatever the source or T cell subsets (Figures S9A and S9B). Approximately 40% of Th0 cells from Rab4b^{flox/flox} mice differentiated in Foxp3⁺ Treg under Treg-polarizing conditions, and a small proportion (~5%) differentiated in IL-17A-producing Th17 (Figure 7D). By contrast, in the same condition, the ability of Th0 cells from Rab4b^{Tcell KO} mice to differentiate into Treg was decreased by ~30%, and the proportion of Th17 was increased by 3-fold

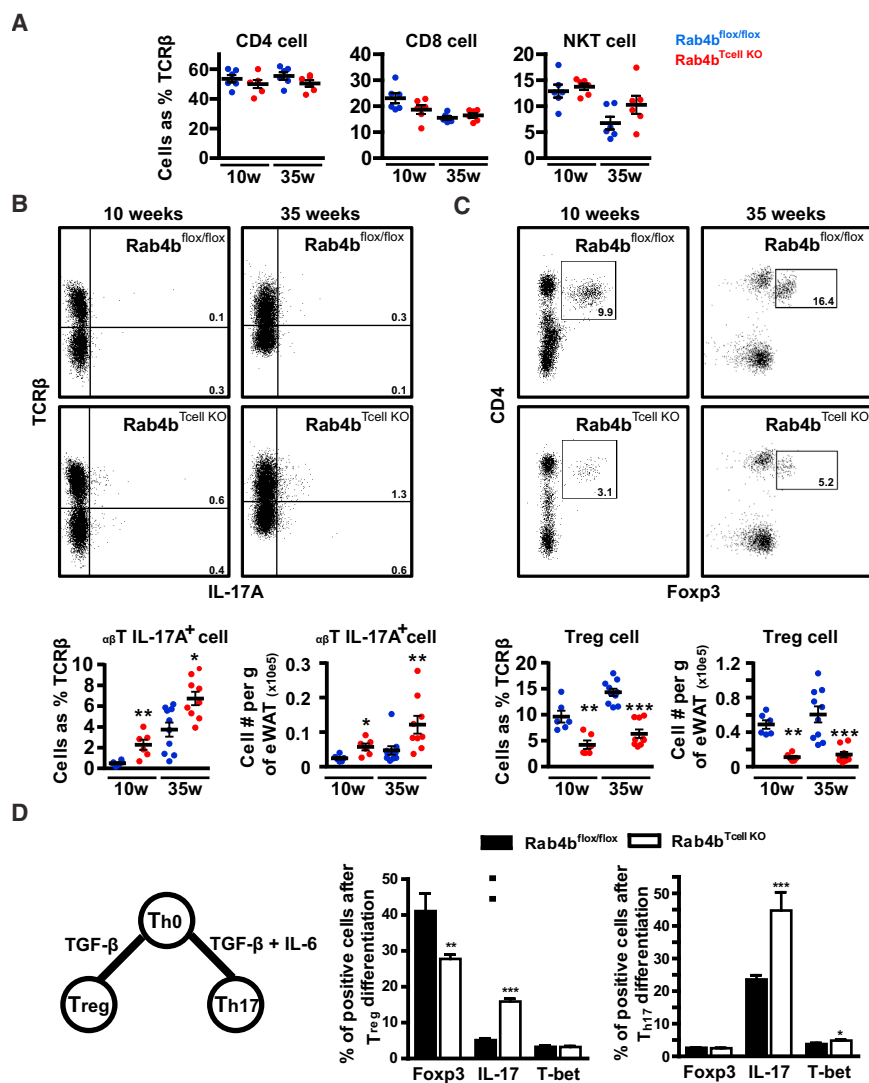


Figure 7. T Cell-Specific Invalidation of Rab4b Alters the Th17/Treg Ratio in EpiWAT and Skews Ex Vivo Th0 Differentiation toward Th17

(A) Frequency of CD4⁺, CD8⁺, and NKT cells among adipose $\alpha\beta$ T cells in epiWAT.

(B) Representative flow cytometry plots and quantification of IL-17A⁺TCR β ⁺ (Th17) cells in epiWAT.

(C) Typical flow cytometry plots and quantification of Fc γ 3⁺CD4⁺ (Treg) in epiWAT. Graphs show the value for each mouse and the means \pm SEMs.

(D) Naive Th0 cells from spleen of 10-week-old Rab4b^{flox/flox} and Rab4b^{Tcell KO} mice were induced to differentiate into Treg (left) or Th17 (right), and the percentage of cells that express Fc γ 3, IL-17A, and T-bet at the end of the differentiation was determined by flow cytometry. Graphs show the means \pm SEMs of Th0 cell differentiation from six different mice per genotype. The experiment was reproduced once with a similar result.

Statistical significance is shown as *p < 0.05, **p < 0.01, and ***p < 0.001.

remodeling, WAT inflammation, and the development of insulin resistance (DiSpirito and Mathis, 2015). We show here that the expression of the small GTPase Rab4b, which is involved in the control of endocytic recycling (Perrin et al., 2013), is decreased in adipose T cells of mice and patients with obesity. Using mice with a specific invalidation of Rab4b in T cells, we report that Rab4b in T cells plays a critical role in the healthy expansion of WAT, in the control of glucose and lipid homeostasis, and in the regulation of WAT Th17 and Treg cell homeostasis.

It is likely that a defect in WAT expandability causes the metabolic dysfunctions

(Figure 7D). The amount of Th1 cells positive for T cell-specific transcription factor (T-bet) was similarly low using Th0 cells either from Rab4b^{flox/flox} or Rab4b^{Tcell KO} mice. Under Th17-polarizing conditions, \sim 45% of Th0 cells from Rab4b^{Tcell KO} mice differentiated into Th17 compared to \sim 25% for Th0 cells from Rab4b^{flox/flox} mice (Figure 7D). The proportion of Th0 cells from Rab4b^{Tcell KO} mice that differentiated into Th1 cells in this condition was also slightly increased compared to Rab4b^{flox/flox} mice (Figure 7D). Our observations thus show that Rab4b deletion in T cell favors Th17 differentiation while repressing Treg cells differentiation in a cell-autonomous manner. This could contribute to the alteration in the Th17/Treg balance in the epiWAT of Rab4b^{Tcell KO} mice.

DISCUSSION

Adaptive immunity is now recognized as an important player in WAT homeostasis. Furthermore, alteration of adipose T cells in WAT from subjects with obesity contributes to pathological WAT

of Rab4b^{Tcell KO} mice. Several studies have shown both in mice and humans with obesity that failure in WAT expandability results in the ectopic fat deposition in muscles and liver that contributes to insulin resistance (Hammarstedt et al., 2018; van Beek et al., 2015). Conversely, proper tissue plasticity and expandability are associated with metabolic health and insulin sensitivity (Arner and Spalding, 2010; Hammarstedt et al., 2018). Chow-fed Rab4b^{Tcell KO} mice consistently display reduced adipogenesis, which is characterized by a decrease in adipocyte number in epiWAT and scWAT and enlarged adipocytes, with an early increase in MSC in epiWAT. This coincides with an increase in circulating NEFA and ectopic fat deposits and the development of glucose intolerance. The adipogenic defect is detectable before the metabolic complications of the Rab4b^{Tcell KO} mice, suggesting that the loss of Rab4b in T cells interferes with healthy WAT development and thus causes the increase in inflammatory macrophages and the metabolic disorder in old chow-fed mice.

The changes in cytokines and chemokines found in the epiWAT of Rab4b^{Tcell KO} mice as early as the age of 10 weeks

certainly drive these pathological steps that are qualitatively reminiscent of the unhealthy development of WAT in obesity. In particular, the loss of Rab4b in T cells increases the production by epiWAT of IL-17A, IL-6, and IL-1, which inhibit adipocyte differentiation (Rotter et al., 2003; Shin et al., 2009; Zúñiga et al., 2010). We also found an increase in CXCL5 and CXCL12 that contributes to obesity-induced inflammation and insulin resistance (Chavey et al., 2009; Kim et al., 2014). Thus, Rab4b invalidation in T cells promotes an early inflammatory state in epiWAT that may restrain the capacity of WAT to properly expand.

The changes in the profile of cytokine and chemokine secretion by the WAT of Rab4b^{Tcell KO} mice certainly result from changes in WAT immune cell content. The lack of Rab4b in T cells results in an early increase in adipose Th17 and a loss of adipose Treg. The increases in Th17 may contribute to the increase in IL-17A secretion since we do not detect changes in IL-17-producing $\gamma\delta$ T or NK cells. We, however, cannot exclude that mucosal-associated invariant T cells (MAITs) or innate lymphoid cell 3 (ILC3) contribute to the production of IL-17A by WAT. These changes in adipose Treg and Th17 are also described during obesity, and the loss of Treg in obesity was causally linked to insulin resistance (Bertola et al., 2012; Dalmás et al., 2014; Eller et al., 2011; Fabbrini et al., 2013; Feuerer et al., 2009; Winer et al., 2009). Also, the frequency of Th17 cells is higher in patients with obesity and type 2 diabetes compared to patients with obesity only, and Th17 can play a pathogenic role in obesity (Chehimi et al., 2017; Dalmás et al., 2014; Fabbrini et al., 2013). The decrease in Rab4b expression is larger in adipose T cells from patients with obesity and diabetes than it is in patients affected by obesity but without diabetes, suggesting a potential association between Rab4b expression in T cells, the number of adipose Th17, and the severity of the metabolic complications of obesity.

The imbalance between adipose Treg and Th17 in the WAT of Rab4b^{Tcell KO} mice strongly suggests that Rab4b in T cells plays a pivotal role in the maintenance of the Treg to Th17 ratio in WAT. Hence, the decrease in Rab4b expression in adipose T cells may participate in the Treg/Th17 imbalance described in WAT during obesity. The mechanisms involved in the increase in Th17 in the WAT of subjects with obesity remain poorly understood, but they could involve several non-exclusive mechanisms. Obesity drives changes in adipocytes, adipose dendritic cells, and adipose stem cells that could more efficiently trigger Th17 differentiation of the WAT resident naive CD4⁺ T cells (Bertola et al., 2012; Chehimi et al., 2017). Obesity is also associated with a splenic and systemic increase in Th17 (DeFuria et al., 2013; Winer et al., 2009) that could yield to parallel variations within tissues. Lastly, the increase in WAT Th17 could result from the transdifferentiation of Treg (Komatsu et al., 2014). We propose that obesity modifies adipose T cells to favor Th17 differentiation and that the decrease in Rab4b expression is involved at the molecular level. Naive T cells from Rab4b^{Tcell KO} mice are prone to differentiate in Th17 when stimulated with anti-CD3/CD28 antibodies in the presence of IL-6 and transforming growth factor β (TGF- β). Thus, the increase in adipose Th17 in Rab4b^{Tcell KO} mice may result from a better intrinsic capacity of T cells to differentiate into Th17 in the presence of small amounts of Th17 inducers in the WAT microenvironment. WAT, even in lean subjects, pro-

duces the Th17 inducers IL-6 and TGF- β (Fain et al., 2005; Gustafson et al., 2007). Accordingly, the IL-6 level is increased in the WAT of Rab4b^{Tcell KO} mice as early as 10 weeks of age. This could later be sustained by the establishment of positive feed-forward loops, since IL-17A secreted by Th17 stimulates the secretion of IL-6 by adipocytes (Shin et al., 2009) and other S_F cell types (Davoine and Lacy, 2014; Ogura et al., 2008).

The lack of Rab4b in T cells also impairs *in vitro* Treg differentiation. Treg and Th17 are reciprocally regulated during differentiation (Ivanov et al., 2007). Thus, our data highlight the pivotal role played by Rab4b in T cells, favoring Treg and restraining Th17 differentiation. However, it is unlikely that the skewing of T cells toward Th17 is the only mechanism involved in the reduced number of adipose Treg in Rab4b^{Tcell KO} mice because the number of Treg decreased 10 times more than the Th17 increased. Alterations in Treg accumulation or survival in WAT are plausible additional mechanisms. In chow-fed mice, adipose Treg cells from the thymus start to expand at the age of 10 weeks (Kolodin et al., 2015), and at this age the number of Treg in the WAT of Rab4b^{Tcell KO} mice is reduced. The number of Treg in WAT relies on the IL-33/ST2 (suppression of tumorigenicity 2) axis and on the TCR-antigen interaction in the MHC class II context (Kolodin et al., 2015; Vasanthakumar et al., 2015). Rab4b plays a role in endocytic trafficking (Perrin et al., 2013), which is involved in the control of the TCR level at the plasma membrane. Moreover, Rab4b co-localizes with intracellular TCR in T cells (Soares et al., 2013), suggesting that Rab4b-dependent pathways regulate TCR trafficking. Rab4b-dependent endocytic processes could also organize an intracellular signaling platform for IL-33 as they did for other cytokines (Cendrowski et al., 2016).

In summary, the present study identified the small GTPase Rab4b in T cells as a key protein contributing to the control of WAT expansion and insulin sensitivity by regulating the adipose Th17/Treg balance. Because the Rab4b level is decreased in adipose T cells of insulin-resistant individuals with obesity, our data suggest that deregulation of Rab4b-dependent endocytic traffic in immune cells may represent an additional mechanism that contributes to the development of obesity-associated metabolic disease.

STAR★METHODS

Detailed methods are provided in the online version of this paper and include the following:

- KEY RESOURCES TABLE
- CONTACT FOR REAGENT AND RESOURCE SHARING
- EXPERIMENTAL MODEL AND SUBJECT DETAILS
 - Human samples
 - Generation of mice with Rab4b invalidation in T lymphocytes
- METHOD DETAILS
 - Material
 - Metabolic exploration of the mice
 - Adipocyte size/number
 - Tissue TG analysis and quantification
 - Adipose mesenchymal stem cell (MSC) and preadipocyte isolation, and adipocyte differentiation

- Identification of cytokines produced by WAT
- Flow cytometry analysis of adipose cells
- Immune cells isolation by magnetic sorting
- *In vitro* T cells differentiation
- Western blotting and RT-qPCR

● **QUANTIFICATION AND STATISTICAL ANALYSIS**

SUPPLEMENTAL INFORMATION

Supplemental Information includes nine figures and three tables and can be found with this article online at <https://doi.org/10.1016/j.celrep.2018.11.083>.

ACKNOWLEDGMENTS

This work was supported by INSERM, the Université Côte d'Azur, a grant from the Société Francophone du Diabète (SFD-MSD 2016) to J.G., and grants from the French National Research Agency (ANR) through the Investments for the Future Labex SIGNALIFE (ANR-11-LABX-0028-01), the program UCA JEDI (ANR-15-IDEX-01), and the Young Investigator Program to J.G. (ANR18-CE14-0035-01-GILLERON). J.G., G.B., and B.V. were supported by fellowships from the Fondation pour la Recherche Médicale, Labex SIGNALIFE, and the French Ministry of Education and Research, respectively. C.M. was supported by a post-doctoral grant from the Ville de Nice. F.C. was supported by a fellowship from INSERM/Région PACA/FEDER and by a grant from the Société Francophone du Diabète. J.-F.T. is an investigator for the Centre National de la Recherche Scientifique (CNRS). N.V. was supported by the European Research Council (ERC-epiFAT-725790). We thank Dr. J. Nunès (INSERM U1068, Marseille) for helpful discussions on T cell biology. We thank M. Gesson from the Imaging Core Facility of C3M funded by the Conseil Général Alpes-Maritimes and Région PACA, which belongs to the IBISA Microscopy and Imaging platform Côte d'Azur (MICA). We also thank V. Corcelle and team from the animal care facility and M. Nebout from the flow cytometry facility at C3M.

AUTHOR CONTRIBUTIONS

M.C. conceived the study and supervised the project. M.C., J.-F.T., and J.G. designed the experiments and analyzed the data. J.G. performed most of the experiments, with G.B., C.M., F.C., B.V., and M.D. for the mice metabolic exploration and S.I. and L.Y.-C. for the flow cytometry analysis of the adipose immune cells. A.J. performed the immune cell magnetic sorting. K.D. performed the indirect calorimetric analyses. N.V. and A.S. supervised the human studies. J.G., J.-F.T., and M.C. wrote the manuscript.

DECLARATION OF INTERESTS

The authors declare no competing interests.

Received: March 20, 2018

Revised: September 4, 2018

Accepted: November 21, 2018

Published: December 18, 2018

REFERENCES

Andersen, C.J., Murphy, K.E., and Fernandez, M.L. (2016). Impact of Obesity and Metabolic Syndrome on Immunity. *Adv. Nutr.* *7*, 66–75.

Angkasekwinai, P., Park, H., Wang, Y.H., Wang, Y.H., Chang, S.H., Corry, D.B., Liu, Y.J., Zhu, Z., and Dong, C. (2007). Interleukin 25 promotes the initiation of proallergic type 2 responses. *J. Exp. Med.* *204*, 1509–1517.

Amer, P., and Spalding, K.L. (2010). Fat cell turnover in humans. *Biochem. Biophys. Res. Commun.* *396*, 101–104.

Bertola, A., Ciucci, T., Rousseau, D., Bourlier, V., Duffaut, C., Bonnafous, S., Blin-Wakkach, C., Anty, R., Iannelli, A., Gugenheim, J., et al. (2012). Identification of adipose tissue dendritic cells correlated with obesity-associated insu-

lin-resistance and inducing Th17 responses in mice and patients. *Diabetes* *61*, 2238–2247.

Bost, F., Aouadi, M., Caron, L., Even, P., Belmonte, N., Prot, M., Dani, C., Hofman, P., Pagès, G., Pouyssegur, J., et al. (2005). The extracellular signal-regulated kinase isoform ERK1 is specifically required for in vitro and in vivo adipogenesis. *Diabetes* *54*, 402–411.

Boutens, L., and Stienstra, R. (2016). Adipose tissue macrophages: going off track during obesity. *Diabetologia* *59*, 879–894.

Cendrowski, J., Mamińska, A., and Miaczynska, M. (2016). Endocytic regulation of cytokine receptor signaling. *Cytokine Growth Factor Rev.* *32*, 63–73.

Chavey, C., Lazennec, G., Lagarrigue, S., Clapé, C., Iankova, I., Teyssier, J., Annicotte, J.S., Schmidt, J., Matak, C., Yamamoto, H., et al. (2009). CXC ligand 5 is an adipose-tissue derived factor that links obesity to insulin resistance. *Cell Metab.* *9*, 339–349.

Chehimi, M., Vidal, H., and Eljaafari, A. (2017). Pathogenic Role of IL-17-Producing Immune Cells in Obesity, and Related Inflammatory Diseases. *J. Clin. Med.* *6*, E68.

Collinet, C., Stöter, M., Bradshaw, C.R., Samusik, N., Rink, J.C., Kenski, D., Habermann, B., Buchholz, F., Henschel, R., Mueller, M.S., et al. (2010). Systems survey of endocytosis by multiparametric image analysis. *Nature* *464*, 243–249.

Cormont, M., Bortoluzzi, M.N., Gautier, N., Mari, M., van Obberghen, E., and Le Marchand-Brustel, Y. (1996). Potential role of Rab4 in the regulation of subcellular localization of Glut4 in adipocytes. *Mol. Cell. Biol.* *16*, 6879–6886.

Crewe, C., An, Y.A., and Scherer, P.E. (2017). The ominous triad of adipose tissue dysfunction: inflammation, fibrosis, and impaired angiogenesis. *J. Clin. Invest.* *127*, 74–82.

Dalmas, E., Venteclef, N., Caer, C., Poitou, C., Cremer, I., Aron-Wisniewsky, J., Lacroix-Desmazes, S., Bayry, J., Kaveri, S.V., Clément, K., et al. (2014). T cell-derived IL-22 amplifies IL-1 β -driven inflammation in human adipose tissue: relevance to obesity and type 2 diabetes. *Diabetes* *63*, 1966–1977.

Dalmas, E., Toubal, A., Alzaid, F., Blazek, K., Eames, H.L., Lebozec, K., Pini, M., Hainault, I., Montastier, E., Denis, R.G., et al. (2015). Irf5 deficiency in macrophages promotes beneficial adipose tissue expansion and insulin sensitivity during obesity. *Nat. Med.* *21*, 610–618.

Davoine, F., and Lacy, P. (2014). Eosinophil cytokines, chemokines, and growth factors: emerging roles in immunity. *Front. Immunol.* *5*, 570.

DeFuria, J., Belkina, A.C., Jagannathan-Bogdan, M., Snyder-Cappione, J., Carr, J.D., Nersesova, Y.R., Markham, D., Strissel, K.J., Watkins, A.A., Zhu, M., et al. (2013). B cells promote inflammation in obesity and type 2 diabetes through regulation of T-cell function and an inflammatory cytokine profile. *Proc. Natl. Acad. Sci. USA* *110*, 5133–5138.

Di Fiore, P.P., and von Zastrow, M. (2014). Endocytosis, signaling, and beyond. *Cold Spring Harb. Perspect. Biol.* *6*, a016865.

DiSpirito, J.R., and Mathis, D. (2015). Immunological contributions to adipose tissue homeostasis. *Semin. Immunol.* *27*, 315–321.

Eller, K., Kirsch, A., Wolf, A.M., Sopper, S., Tagwerker, A., Stanzl, U., Wolf, D., Patsch, W., Rosenkranz, A.R., and Eller, P. (2011). Potential role of regulatory T cells in reversing obesity-linked insulin resistance and diabetic nephropathy. *Diabetes* *60*, 2954–2962.

Fabbrini, E., Cella, M., McCartney, S.A., Fuchs, A., Abumrad, N.A., Pietka, T.A., Chen, Z., Finck, B.N., Han, D.H., Magkos, F., et al. (2013). Association between specific adipose tissue CD4+ T-cell populations and insulin resistance in obese individuals. *Gastroenterology* *145*, 366–374.e-3.

Fain, J.N., Tichansky, D.S., and Madan, A.K. (2005). Transforming growth factor beta1 release by human adipose tissue is enhanced in obesity. *Metabolism* *54*, 1546–1551.

Fan, R., Toubal, A., Goñi, S., Drareni, K., Huang, Z., Alzaid, F., Ballaire, R., Ancel, P., Liang, N., Damdimopoulos, A., et al. (2016). Loss of the co-repressor GPS2 sensitizes macrophage activation upon metabolic stress induced by obesity and type 2 diabetes. *Nat. Med.* *22*, 780–791.

Feuerer, M., Herrero, L., Cipolletta, D., Naaz, A., Wong, J., Nayer, A., Lee, J., Goldfine, A.B., Benoist, C., Shoelson, S., and Mathis, D. (2009). Lean, but

- not obese, fat is enriched for a unique population of regulatory T cells that affect metabolic parameters. *Nat. Med.* 15, 930–939.
- Fitzgibbons, T.P., and Czech, M.P. (2016). Emerging evidence for beneficial macrophage functions in atherosclerosis and obesity-induced insulin resistance. *J. Mol. Med. (Berl.)* 94, 267–275.
- Frayne, K.N. (1983). Calculation of substrate oxidation rates in vivo from gaseous exchange. *J. Appl. Physiol.* 55, 628–634.
- Galvez, T., Gilleron, J., Zerial, M., and O'Sullivan, G.A. (2012). SnapShot: mammalian Rab proteins in endocytic trafficking. *Cell* 151, 234–234.e2.
- Guo, K.Y., Halo, P., Leibel, R.L., and Zhang, Y. (2004). Effects of obesity on the relationship of leptin mRNA expression and adipocyte size in anatomically distinct fat depots in mice. *Am. J. Physiol. Regul. Integr. Comp. Physiol.* 287, R112–R119.
- Gurkan, C., Lapp, H., Alory, C., Su, A.I., Hogenesch, J.B., and Balch, W.E. (2005). Large-scale profiling of Rab GTPase trafficking networks: the membrane. *Mol. Biol. Cell* 16, 3847–3864.
- Gustafson, B., Hammarstedt, A., Andersson, C.X., and Smith, U. (2007). Inflamed adipose tissue: a culprit underlying the metabolic syndrome and atherosclerosis. *Arterioscler. Thromb. Vasc. Biol.* 27, 2276–2283.
- Hammarstedt, A., Gogg, S., Hedjazifaz, S., Nerstedt, A., and Smith, U. (2018). Impaired Adipogenesis and Dysfunctional Adipose Tissue in Human Hypertrophic Obesity. *Physiol. Rev.* 98, 1911–1941.
- Han, S.J., Glatman Zaretsky, A., Andrade-Oliveira, V., Collins, N., Dzutsev, A., Shaik, J., Morais da Fonseca, D., Harrison, O.J., Tamoutounour, S., Byrd, A.L., et al. (2017). White Adipose Tissue Is a Reservoir for Memory T Cells and Promotes Protective Memory Responses to Infection. *Immunity* 47, 1154–1168.e6.
- He, J., Usui, I., Ishizuka, K., Kanatani, Y., Hiratani, K., Iwata, M., Bukhari, A., Haruta, T., Sasaoka, T., and Kobayashi, M. (2006). Interleukin-1 α inhibits insulin signaling with phosphorylating insulin receptor substrate-1 on serine residues in 3T3-L1 adipocytes. *Mol. Endocrinol.* 20, 114–124.
- Ivanov, I.I., Zhou, L., and Littman, D.R. (2007). Transcriptional regulation of Th17 cell differentiation. *Semin. Immunol.* 19, 409–417.
- Jo, J., Gavrilova, O., Pack, S., Jou, W., Mullen, S., Sumner, A.E., Cushman, S.W., and Perival, V. (2009). Hypertrophy and/or Hyperplasia: Dynamics of Adipose Tissue Growth. *PLoS Comput. Biol.* 5, e1000324.
- Kaddai, V., Gonzalez, T., Keslair, F., Grémeaux, T., Bonnafous, S., Gugenheim, J., Tran, A., Gual, P., Le Marchand-Brustel, Y., and Cormont, M. (2009). Rab4b is a small GTPase involved in the control of the glucose transporter GLUT4 localization in adipocyte. *PLoS One* 4, e5257.
- Kim, D., Kim, J., Yoon, J.H., Ghim, J., Yea, K., Song, P., Park, S., Lee, A., Hong, C.P., Jang, M.S., et al. (2014). CXCL12 secreted from adipose tissue recruits macrophages and induces insulin resistance in mice. *Diabetologia* 57, 1456–1465.
- Kolodin, D., van Panhuys, N., Li, C., Magnuson, A.M., Cipolletta, D., Miller, C.M., Wagers, A., Germain, R.N., Benoist, C., and Mathis, D. (2015). Antigen- and cytokine-driven accumulation of regulatory T cells in visceral adipose tissue of lean mice. *Cell Metab.* 21, 543–557.
- Komatsu, N., Okamoto, K., Sawa, S., Nakashima, T., Oh-hora, M., Kodama, T., Tanaka, S., Bluestone, J.A., and Takayanagi, H. (2014). Pathogenic conversion of Foxp3⁺ T cells into TH17 cells in autoimmune arthritis. *Nat. Med.* 20, 62–68.
- Mari, M., Monzo, P., Kaddai, V., Keslair, F., Gonzalez, T., Le Marchand-Brustel, Y., and Cormont, M. (2006). The Rab4 effector Rabip4 plays a role in the endocytic trafficking of Glut 4 in 3T3-L1 adipocytes. *J. Cell Sci.* 119, 1297–1306.
- Ogura, H., Murakami, M., Okuyama, Y., Tsuruoka, M., Kitabayashi, C., Kanamoto, M., Nishihara, M., Iwakura, Y., and Hirano, T. (2008). Interleukin-17 promotes autoimmunity by triggering a positive-feedback loop via interleukin-6 induction. *Immunity* 29, 628–636.
- Pei, G., Bronietzki, M., and Gutierrez, M.G. (2012). Immune regulation of Rab proteins expression and intracellular transport. *J. Leukoc. Biol.* 92, 41–50.
- Pellegrinelli, V., Carobbio, S., and Vidal-Puig, A. (2016). Adipose tissue plasticity: how fat depots respond differently to pathophysiological cues. *Diabetologia* 59, 1075–1088.
- Perrin, L., Lacas-Gervais, S., Gilleron, J., Ceppo, F., Prodon, F., Benmerah, A., Tanti, J.F., and Cormont, M. (2013). Rab4b controls an early endosome sorting event by interacting with the γ -subunit of the clathrin adaptor complex 1. *J. Cell Sci.* 126, 4950–4962.
- Priceman, S.J., Kujawski, M., Shen, S., Cherryholmes, G.A., Lee, H., Zhang, C., Kruper, L., Mortimer, J., Jove, R., Riggs, A.D., and Yu, H. (2013). Regulation of adipose tissue T cell subsets by Stat3 is crucial for diet-induced obesity and insulin resistance. *Proc. Natl. Acad. Sci. USA* 110, 13079–13084.
- Rink, J., Ghigo, E., Kalaidzidis, Y., and Zerial, M. (2005). Rab conversion as a mechanism of progression from early to late endosomes. *Cell* 122, 735–749.
- Rotter, V., Nagaev, I., and Smith, U. (2003). Interleukin-6 (IL-6) induces insulin resistance in 3T3-L1 adipocytes and is, like IL-8 and tumor necrosis factor- α , overexpressed in human fat cells from insulin-resistant subjects. *J. Biol. Chem.* 278, 45777–45784.
- Rouault, C., Pellegrinelli, V., Schilch, R., Cotillard, A., Poitou, C., Tordjman, J., Sell, H., Clément, K., and Lacasa, D. (2013). Roles of chemokine ligand-2 (CXCL2) and neutrophils in influencing endothelial cell function and inflammation of human adipose tissue. *Endocrinology* 154, 1069–1079.
- Rutkowski, J.M., Stern, J.H., and Scherer, P.E. (2015). The cell biology of fat expansion. *J. Cell Biol.* 208, 501–512.
- Shin, J.H., Shin, D.W., and Noh, M. (2009). Interleukin-17A inhibits adipocyte differentiation in human mesenchymal stem cells and regulates pro-inflammatory responses in adipocytes. *Biochem. Pharmacol.* 77, 1835–1844.
- Soares, H., Henriques, R., Sachse, M., Ventimiglia, L., Alonso, M.A., Zimmer, C., Thoulouze, M.I., and Alcover, A. (2013). Regulated vesicle fusion generates signaling nanoterritories that control T cell activation at the immunological synapse. *J. Exp. Med.* 210, 2415–2433.
- Tanti, J.F., Ceppo, F., Jager, J., and Berthou, F. (2013). Implication of inflammatory signaling pathways in obesity-induced insulin resistance. *Front. Endocrinol. (Lausanne)* 3, 181.
- van Beek, L., van Klinken, J.B., Pronk, A.C., van Dam, A.D., Dirven, E., Rensen, P.C., Koning, F., Willems van Dijk, K., and van Harmelen, V. (2015). The limited storage capacity of gonadal adipose tissue directs the development of metabolic disorders in male C57Bl/6J mice. *Diabetologia* 58, 1601–1609.
- Vasanthakumar, A., Moro, K., Xin, A., Liao, Y., Gloury, R., Kawamoto, S., Fagarasan, S., Mielke, L.A., Afshar-Sterle, S., Masters, S.L., et al. (2015). The transcriptional regulators IRF4, BATF and IL-33 orchestrate development and maintenance of adipose tissue-resident regulatory T cells. *Nat. Immunol.* 16, 276–285.
- Vergoni, B., Cornejo, P.J., Gilleron, J., Djedaini, M., Ceppo, F., Jacquet, A., Bouget, G., Ginet, C., Gonzalez, T., Maillat, J., et al. (2016). DNA Damage and the Activation of the p53 Pathway Mediate Alterations in Metabolic and Secretory Functions of Adipocytes. *Diabetes* 65, 3062–3074.
- Winer, S., Chan, Y., Paltser, G., Truong, D., Tsui, H., Bahrami, J., Dorfman, R., Wang, Y., Zielinski, J., Mastronardi, F., et al. (2009). Normalization of obesity-associated insulin resistance through immunotherapy. *Nat. Med.* 15, 921–929.
- Zúñiga, L.A., Shen, W.J., Joyce-Shaikh, B., Pyatnova, E.A., Richards, A.G., Thom, C., Andrade, S.M., Cua, D.J., Kraemer, F.B., and Butcher, E.C. (2010). IL-17 regulates adipogenesis, glucose homeostasis, and obesity. *J. Immunol.* 185, 6947–6959.

STAR★METHODS

KEY RESOURCES TABLE

REAGENT or RESOURCE	SOURCE	IDENTIFIER
Antibodies		
Home-made rabbit polyclonal anti-Rab4b (immunized with C-terminal part of Rab4b)	Perrin et al., 2013, and this paper	N/A
Mouse monoclonal anti-ERK2 (clone D2)	Santa Cruz Biotechnology	Cat# sc-1647; RRID: AB_627547
Rabbit monoclonal anti-ERK1/2 (clone 137F5)	Cell Signaling Technology	Cat# 4695; RRID: AB_390779
Rabbit monoclonal anti-phospho-AKT T308 (clone D25E6)	Cell Signaling Technology	Cat# 13038; RRID: AB_2629447
Rabbit monoclonal anti-phospho-AKT S473 (clone D9E)	Cell Signaling Technology	Cat# 4060; RRID: AB_2315049
Rabbit polyclonal anti-phospho-HSL S563	Cell Signaling Technology	Cat# 4139; RRID: AB_2135495
Peroxidase AffiniPure Goat polyclonal Anti-Rabbit IgG	Jackson ImmunoResearch	Cat# 111-035-144; RRID: AB_2307391
Peroxidase AffiniPure Goat polyclonal Anti-Mouse IgG	Jackson ImmunoResearch	Cat# 115-035-205; RRID: AB_2338513
CD3 (clone 145-2C11)	BD Bioscience	Cat# 553058; RRID: AB_394591
CD28 (clone 37.51)	BD Bioscience	Cat# 553295; RRID: AB_394764
CD11c-APC (clone N418)	eBioscience	Cat# 17-0114-82; RRID: AB_469346
F4/80-PE (clone BM8)	eBioscience	Cat# 12-4801-82; RRID: AB_465923
CD44-PE_Cy7 (clone IM7)	eBioscience	Cat# 25-0441-81; RRID: AB_469622
Foxp3-Alexa647 (clone FJK165)	eBioscience	Cat# 51-5773-82; RRID: AB_763538
CD8-FITC (clone H35-17.2)	eBioscience	Cat# 11-0083-85; RRID: AB_657766
CD45-APC_Cy7 (clone 30-F11)	BD Bioscience	Cat# 557659; RRID: AB_396774
TCRβ-PB (clone H57-597)	BD Bioscience	Cat# 109226; RRID: AB_1027649
CD4-Percp_Cy5.5 (clone RM4-4)	BD Bioscience	Cat# 116012; RRID: AB_2563023
CD8-PE_Cy7 (clone 53-6.7)	BD Bioscience	Cat# 552877; RRID: AB_394506
CD19-Alexa647 (clone 6D5)	BD Bioscience	Cat# 115522; RRID: AB_389329
NK1.1-FITC (clone PK136)	BD Bioscience	Cat# 108706; RRID: AB_313393
CD4-FITC (clone RM4-5)	BD Bioscience	Cat# 100510; RRID: AB_312713
CD62L-APC (clone MEL-14)	BD Bioscience	Cat# 104411; RRID: AB_313098
CD69-PE	BD Bioscience	Cat# 553237; RRID: AB_394726
Fc Block 2-4G2 (clone 2.4G2)	BD Bioscience	Cat# 553142; RRID: AB_394657
IL17-APC	Miltenyi Biotech	Cat# 130-102-298; RRID: AB_2660790
TCRγδ-PE	Miltenyi Biotech	Cat# 130-104-012; RRID: AB_2654078
Chemicals, Peptides, and Recombinant Proteins		
Dulbecco's modified Eagle's medium (DMEM)	GIBCO	Cat# 41965-039
Fetal Calf Serum	GIBCO	Cat# 10270-106
New born Serum	GIBCO	Cat# 16010-159
Penicillin/Streptomycin	GIBCO	Cat# 15140-122
Gentamycin	GIBCO	Cat# 15710-049
MesenCult Medium	Stem Cell Technologies	Cat# 05502
Isobutylmethylxantine	Sigma	Cat# I5879
Dexamethasone	Sigma	Cat# D4902
Rosiglitazone	Enzo Life Science	Cat# ALX-350-125
Insulin	GIBCO	Cat# 12585-014
Collagenase	Sigma	Cat# C6885
Acrylamide/Bis-Acrylamide 37.5:1 40%	Biosolve	Cat# 01422301
Trizol	Life Technology	Cat# 15596018

(Continued on next page)

Continued

REAGENT or RESOURCE	SOURCE	IDENTIFIER
Tris	Euromedex	Cat# 261283094A
Permeabilisation buffer	eBioscience	Cat# 00-8333-56
Fixation buffer diluent	eBioscience	Cat# 00-5223-56
Fixation buffer concentrate	eBioscience	Cat# 00-5123-43
Oil red O	Sigma	Cat# O0625
Crystal Violet stain	Sigma	Cat# C3886
Hematoxylin	MM France	Cat# F/HAQ500
Eosin Y	MM France	Cat# F/C0352
IL-4	R&D Systems	Cat# 404-ML
IL-12	R&D Systems	Cat# 419-ML
IL-6	R&D Systems	Cat# 406-ML
TGF β	R&D Systems	Cat# 7666-MB
IL-2	R&D Systems	Cat# 402-ML
Critical Commercial Assays		
Insulin ultra-sensitiv assay kit HTRF	CisBio	Cat# 62IN3PEB
NEFA standard FS DiaSys assay kit	Diagnostic Systems	# 1 578199 10935
DiaSys triglyceride assay kit	Diagnostic Systems	# 1 571099 10021
Cytokine and/or chemokine array panel A	R&D Systems	Cat# ARY006
Reverse transcription AMV RT Kit	Promega	Cat# A3500
Sybr Green PCR master Mix kit	Applied Biosystems	Cat# 4344463
Substrat HRP immobilon ECL kit	Millipore	Cat# WBKLS0500
Naive CD4 ⁺ T cell Isolation kit (mouse)	Miltenyi Biotech	Cat# 130-104-453
Anti-PE microbeads	Miltenyi Biotech	Cat# 130-048-801
Experimental Models: Cell Lines		
3T3-L1 fibroblast	ATCC	ATCC CL-173
Experimental Models: Organisms/Strains		
B6-Tg(Rab4b-flox)/N mice	Institut Clinique de la Souris (ICS, Illkirch, France)	N/A
B6-Tg(Lck-cre)/J mice	Jackson Laboratories	strain 3802
Oligonucleotides		
See Table S3 for oligonucleotide sequences		N/A
Software and Algorithms		
FlowJo	Tree Star	N/A
MACSQuantify	Miltenyi Biotech	N/A
Motion Tracking	Generously provided by Yannis Kalaidzidis from Marino Zerial Lab (MPI-CBG Dresden)	N/A
FiJi (ImageJ image analysis software)	Freeware from the NIH	N/A
GraphPad Prism 7	GraphPad Software	N/A
Multi Gauge V3.0 software	FujiFilm software	N/A
Other		
Regular Chow Diet (ND)	SAFE custom diet	Cat# A04
High Fat Diet 60% (HFD)	SAFE custom diet	Cat# 230HF

CONTACT FOR REAGENT AND RESOURCE SHARING

Further information and requests for resources and reagents should be directed to and will be fulfilled by the Lead Contact, Dr. Mireille Cormont (cormont@unice.fr).

EXPERIMENTAL MODEL AND SUBJECT DETAILS

Human samples

Subjects were composed of patients affected by morbid obesity eligible for laparoscopic Roux-en-Y gastric bypass surgery and are included in a larger cohort described in (Dalmas et al., 2015; Fan et al., 2016). Subjects with obesity were segregated in nondiabetic and type 2 diabetic patients based on fasting glycemia over 7 mmol/L or use of antidiabetic drugs. Control subjects without obesity involved in programmed surgery for hernia, nissen fundoplication, or gallbladder ablation were included and selected without dyslipidemia, type 2 diabetes, or chronic inflammatory or infectious diseases. The subjects were recruited at Geoffroy Saint-Hilaire Clinique (Ramsey Générale de Santé), Paris, France. The study was conducted in accordance with the Helsinki and the Ethics Committee (CPP Ile-de-France) approved the clinical investigations for individuals with or without obesity. All subjects provided written informed consent when included in the surgery program. Characteristics of the subjects are shown in Table S1.

Generation of mice with Rab4b invalidation in T lymphocytes

The studies with mice were conducted in accordance with the European and French guidelines and approved by our animal care committee CIEPAL-AZUR (number: NCE/2013-83). C57BL/6N Rab4b^{flox/flox} mice were obtained under pure background at the Mouse Clinical Institute (ICS, Illkirch, France) as schematized in Figure 2. Rab4b^{flox/flox} were crossed with mice expressing the Cre recombinase under the Lck promoter to obtain Lck-Cre Rab4b^{flox/wt} mice. The obtained mice were crossed together to select Lck-Cre-Rab4b^{flox/flox} mice. They were then crossed with Rab4b^{flox/flox} mice to generate in the same littermate mice invalidated for Rab4b in T lymphocytes (Rab4b^{Tcell KO} mice) and Rab4b^{flox/flox} mice as control. When mentioned, other control mice (wild-type and Lck-cre) were selected in the crossing of Lck-Cre-Rab4b^{flox/wt} with themselves. The Rab4b^{Tcell KO} mice were viable and born at expected Mendelian ratio. Male mice were used for the study.

The genotyping of the mice was performed on DNA from tails using the following primers: to detect Rab4b with flox sequences 5'-TGGCACTTCCAGCAGTGGGT-3' and 5'-TTCCCCTGCCTCTTCTGCCC-3' (Figure S1A), with the following reaction procedure: 3 min at 94°C / 5 cycles of 1 min at 94°C, 1 min at 62°C, 1 min at 72°C / 40 cycles of 10sec at 94°C, 30 s at 62°C, 1 min at 72°C / 3min at 72°C. To detect the Cre-recombinase 5'-CGA TGC AAC GAG TGA TGA GGT TC-3' and 5'-GCA CGT TCA CCG GCA TCA AC-3' according to The Jackson Laboratories' procedure.

METHOD DETAILS

Material

Flow cytometers

T cell subtypes were analyzed using a BD FACSCanto analyzer (Becton Dickinson) and FlowJo software (Tree Star). Myeloid cells were analyzed using MACSQuant Analysers and MACSQuantify software (Miltenyi Biotech) as described in (Vergoni et al., 2016). Magnetic sorting was performed using an AutoMacs Pro separator, Miltenyi Biotech.

Microscopes

Zeiss PALM Micro Beam system equipped with Plan-Neofluar 10x (0.3 N.A.) air objective and an AxioCam MRc5 color camera; Nikon Eclipse Ci equipped with Plan-Neofluar 10x (0.25 N.A.) and Plan-Neofluar 20x (0.4 N.A.) and a Nikon color camera (C3M light microscopy facility, MiCA Ibis platform, Nice).

Metabolic exploration of the mice

Mice were housed in a 23°C on a 12 h light-dark cycle in the animal facility of the INSERM U1065 (Nice, France). Male mice were fed NCD or 60% HFD from 7-8 weeks of age.

Intraperitoneal glucose tolerance tests (IPGTT; 0.8 g/kg body weight) and intraperitoneal insulin tolerance test (0.75 U/kg body weight) were performed in 6-hr fasted mice. Glucose level was measured in tail vein blood using a glucometer (FreeStyle Optium, Abbott Laboratories, Abbott Park, USA). Serum insulin and NEFAs were measured using an HTRF-based or biochemical assay, respectively.

Mice metabolism were analyzed by indirect calorimetry to determine oxygen consumption (VO₂) and carbon dioxide production (VCO₂), energy expenditure, respiratory quotient ([RQ] = VCO₂/VO₂), and locomotor activity using calorimetric tides cages (Oxylet-pro-Physiocage Panlab, Bioseb, Vitrolles, France). For that, mice were individually housed and acclimated for 24 h before experimental measurements. Analysis was first performed during 24 h with mice having free access to food and water. The equations of Frayn (Frayn, 1983) were used to calculate the energy expenditure (EE; in kcal/day/kg^{0.75} = [3.815 + (1.232 x RQ)] x 1.44 x VO₂).

Adipocyte size/number

WAT was fixed in 4% PFA and embedded in paraffin. The WAT sections stained with hematoxylin-eosin were imaged on a Zeiss PALM MicroBeam system. Five images were randomly captured per sections and the diameters of adipocytes were semi-automatically counted by using a plug-in developed by Dr G. Marsico on Motion Tracking software. At least 10000 adipocytes were counted per conditions.

To estimate the number of adipocytes in whole WAT depots mice, we applied the mathematical equation developed by Jo and Colleagues (Jo et al., 2009). Briefly, the number of adipocytes (N) was estimated by dividing the WAT mass (M) by the density of adipocytes ($D = 0.915$ g/L) multiplied by the mean volume of adipocytes within the WAT (V). The mean volume of adipocytes is calculated from the mean diameters of adipocytes (see above). The equation is presented below:

$$N = \frac{M}{D \left(\frac{4}{3} \pi R^3 \right)}$$

Tissue TG analysis and quantification

For tissue triglyceride (TG) quantification, snap-frozen liver or muscles were homogenized in sodium acetate (0.2M, pH 4.5) using a Precellys Homogenizer and centrifuged. Supernatants were collected, and TG content quantified using the DiaSys triglyceride assay kit.

For liver section oil red O staining, 10 μ m liver tissue sections were labeled using oil red O (3 g/l in 60% isopropanol) and imaged using a Zeiss PALM Micro Beam system. Quantification of the number and the size of the lipid droplets was performed using MotionTracking quantitative multiparametric image analysis platform (Collinet et al., 2010; Rink et al., 2005) on 30 randomly captured images per condition.

Adipose mesenchymal stem cell (MSC) and preadipocyte isolation, and adipocyte differentiation

Stromal vascular fraction (S_F) from epiWAT of 10-week-old mice was obtained by collagenase digestion (Cormont et al., 1996). MSC were obtained by plating the S_F and cultivating it in MesenCult medium with antibiotics. The culture of MSC in MesenCult medium for 14 days in condition of limit dilutions allowed for their number quantification. Mouse pre-adipocytes were obtained from S_F (Bost et al., 2005).

Adipocyte differentiation was then induced. Briefly, adipose MSC, pre-adipocytes and 3T3-L1 cells were cultured in MesenCult medium or DMEM, respectively, until 2-days post-confluence. They were then differentiated into adipocyte using 5 μ g/ml insulin, 0.25 μ M dexamethasone, and 0.5 mM isobutyl methylxanthine for two days. The medium was then changed for the same medium containing insulin for two additional days. Then the cells were cultured for 3 days in the appropriate medium without insulin. All the culture media were supplemented with 1% penicillin/ streptomycin/gentamycin.

The impact of WAT secretome on adipocyte differentiation was tested by adding during the first two days of 3T3-L1 differentiation freshly harvested WAT explants (~200 mg) from 10-week-old mice in a Boyden chamber.

The extent of differentiation was analyzed by quantification of the expression of adipocyte genes using RT-qPCR and using oil red O to label lipid droplets and DAPI to label the nuclei. We collected fluorescent images of lipids (from oil red O staining using the alexa555 filters set) and DAPI (using the alexa405 filter set). Then the areas covered by lipid droplets were normalized by the number of nuclei. For the quantification of mesenchymal stem cells in adipose tissue S_F were prepared from individual mice and were cultured in as recommended by the manufacturer.

Identification of cytokines produced by WAT

EpiWAT explants from four 10-week-old Rab4b^{flox/flox} mice and four Rab4b^{Tcell KO} mice were cultured in DMEM containing 10% fetal calf serum, 1% penicillin/streptomycin/gentamycin. 24 h later, the conditioned media were applied on cytokine and/or chemokine array membranes then treated according to the manufacturer.

Flow cytometry analysis of adipose cells

The S_F from WAT was obtained following collagenase digestion and the number of cells determined. Staining procedures and gating strategy were applied on 2×10^6 S_F cells (Figure S5) and the cells were subjected to flow cytometry analysis.

For the analysis of adipose myeloid cells, freshly isolated cells from S_F were labeled with F4/80-PE (100 $^\circ$) and CD11c-APC (100 $^\circ$) for 30 min at 4 $^\circ$ C. After washes, the cells were analyzed by flow cytometry.

For the analysis of adipose T cells, three staining procedures were used. For the staining procedure 1 (Figure S5B), cells were labeled at 4 $^\circ$ C for 30 min with Fc Block 2-4G2 (50 $^\circ$) and the indicated fluorescently-coupled antibodies: CD45-APC_Cy7 (200 $^\circ$), TCR β -PB (100 $^\circ$), TCR $\gamma\delta$ -PE (50 $^\circ$), CD4-Percp_Cy5.5 (100 $^\circ$), CD8-PE_Cy7 (200 $^\circ$), CD19-APC (200 $^\circ$) and NK1.1-FITC (200 $^\circ$). For the staining procedure 2 (Figure S5C), cells were labeled at 4 $^\circ$ C for 30 min with the Fc Block 2-4G2 (50 $^\circ$) and the following labeled-antibodies: CD45-APC_Cy7 (200 $^\circ$), TCR β -PB (100 $^\circ$) and CD4-Percp_Cy5.5 (100 $^\circ$). After two washes, the cells were incubated for 30 min on ice in a fixation/permeabilization buffer. Following two washes, cells were incubated for 30 min at room temperature with Foxp3-APC (100 $^\circ$) and the Fc Block 2-4G2 (50 $^\circ$). For the staining procedure 3 (Figure S5D), cells were first maintained at 37 $^\circ$ C for 4 h in T cell culture media supplemented with 50 ng/ml of PMA, 500 ng/ml of ionomycin and 0.6 μ l/ml of Golgi stop (Angkasekwina et al., 2007). Then, they were labeled at 4 $^\circ$ C for 30 min with anti CD45-APC_Cy7 (200 $^\circ$), TCR β -PB (100 $^\circ$), TCR $\gamma\delta$ -PE (50 $^\circ$), CD4-FITC (100 $^\circ$), NK1.1-PE_Cy7 (50 $^\circ$), and the Fc Block 2-4G2 (50 $^\circ$). The cells were washed twice and incubated with the fixation/permeabilization buffer for 30 min on ice. Cells were then washed twice and incubated for 30 min at room temperature with

IL17-APC (50°) and the Fc Block 2-4G2 (50°). This procedure was complemented using CD4-PercP_Cy5.5 (100°) and CD8-FITC (200°) to determine the proportion of TCRβ⁺CD4⁺ and TCRβ⁺CD8⁺ cells that express IL-17A.

For the analysis of memory T cells, freshly isolated cell from the S_F were incubated with anti CD45-APC_Cy7 (200°), TCRβ-PB (100°), CD4-PercP_Cy5.5 (100°), CD8-FITC (200°), CD62L-APC (200°), CD69-PE (100°), CD44-PE_Cy7 (200°) and the Fc Block 2-4G2 (50°) for 30 min at 4°C.

Immune cells isolation by magnetic sorting

Mouse CD3⁺ cells were enriched from S_F cells or fresh thymocytes by positive magnetic sorting on cells incubated with anti CD3-PE antibody and anti-PE antibody coupled with magnetic beads. Human CD3⁺ cells were enriched from VAT S_F purified as described (Rouault et al., 2013) using magnetic beads as in (Dalmas et al., 2015).

Mouse B cells and NK/NKT cells were enriched from freshly mechanically dissociated cells from spleen using PE-labeled antibody directed against B220 or NK1.1, respectively, and anti-PE antibody coupled with magnetic beads before positive magnetic sorting. Mouse monocytes were enriched from freshly prepared bone marrow cells using PE-labeled antibody directed against CD11b and sorted as above.

In vitro T cells differentiation

Naive CD4⁺ T cells from spleen (CD4⁺CD62L^{high}CD44^{low}) obtained by using a naive CD4⁺ isolation kit with a magnetic cell sorter were activated by plating them on 24-well plates pre-coated with antibodies against CD3 (10 μg/ml) in RPMI with 5% fetal calf serum, 1% penicillin/streptomycin and 50 μM β-mercapto-ethanol containing soluble CD28 (2 μg/ml). Their differentiation were induced into Treg cells with IL-2 (20 ng/ml) and TGF-β (1 ng/ml), or into Th17 cells with TGF-β (1 ng/ml) and IL-6 (100 ng/ml), or into Th1 with IL-2 (20 ng/ml) and IL-12 (20 ng/ml). After 5 days of treatment, the efficiency in Th17 or Treg cell differentiation was estimated by quantifying the expression of markers of T cell subpopulations by flow cytometry.

Western blotting and RT-qPCR

Snap frozen tissues were lysed, and immunoblotting was performed using the indicated antibodies as described (Kaddai et al., 2009). Detection was made using ECL (Millipore, Molsheim, France) and incremental images were acquired on an ImageQuant LAS 4000 (GE Healthcare Life Sciences) and quantifications were performed with Multi Gauge V3.0 software.

RNAs were prepared from snap-frozen tissues using TRIzol and RT-qPCR were performed as previously (Kaddai et al., 2009). Primer sequences are provided in Table S3. The qPCR reactions were performed using StepOne devices from Applied Biosystems (Thermo Fisher Scientific, Illkirch, France), and the PCR data were normalized to mouse *Rplp0* gene expression and the comparative Ct (ΔΔCt) quantitation method was used.

QUANTIFICATION AND STATISTICAL ANALYSIS

Data are presented as the mean ± SEM. Statistical significance between two groups of mice was evaluated with Mann-Whitney test. Statistical significance between the different time points was assessed by two-way ANOVA followed by post hoc comparison. A p value < 0.05 was considered statistically significant. All statistical details of experiments can be found in the figure legends. GraphPad PRISM5 software was used.